

UC Irvine

UC Irvine Previously Published Works

Title

PEM-West A: Meteorological overview

Permalink

<https://escholarship.org/uc/item/9zn3z84t>

Journal

Journal of Geophysical Research, 101(D1)

ISSN

0148-0227

Authors

Bachmeier, A Scott
Newell, Reginald E
Shipham, Mark C
[et al.](#)

Publication Date

1996-01-20

DOI

10.1029/95jd02799

Copyright Information

This work is made available under the terms of a Creative Commons Attribution License, available at <https://creativecommons.org/licenses/by/4.0/>

Peer reviewed

PEM-West A: Meteorological overview

A. Scott Bachmeier,¹ Reginald E. Newell,² Mark C. Shipham,³ Yong Zhu,²
Donald R. Blake,⁴ and Edward V. Browell³

Abstract. Phase A of the NASA Pacific Exploratory Mission in the western North Pacific (PEM-West A) region was conducted during September-October 1991. The background meteorology of eastern Asia and the western North Pacific region during the PEM-West A study is described. Mean large-scale flow patterns are discussed along with transient synoptic scale features (e.g., midlatitude cyclones, anticyclones, and frontal systems) responsible for long-range transport of trace species over the study region. Synoptic summaries are given for each of the 18 data flights, together with selected examples of meteorological processes that gave rise to some of the changes observed in the measured trace gases. Examples of large-scale ozone features observed above and below the DC-8 flight altitude by an onboard lidar system are also related to meteorological processes such as stratospheric-tropospheric exchange and upward transport of air from the boundary layer.

1. Introduction

The broad objectives of the National Aeronautics and Space Administration's (NASA) Pacific Exploratory Mission in the western North Pacific (PEM-West) region are to study the chemical processes and long-range transport of trace gas species over the Pacific Ocean and to estimate the human impact on chemistry of the troposphere in this region. Specifically, the major objectives of PEM-West are to understand the factors influencing the budgets of ozone and sulfur. The overall experimental design of PEM-West encompassed two intensive airborne field studies positioned in time such that contrasting meteorological regimes in the western North Pacific could be sampled. The first phase, PEM-West A, was conducted during September-October 1991, a period in which the lower tropospheric airflow was dominated by flow from the mid-Pacific regions. The phase B was conducted in March 1994, a period characterized by maximum outflow from the Asian continent.

During PEM-West A, a large suite of atmospheric trace gases was measured by instruments aboard the NASA DC-8 aircraft. A total of 18 flights were conducted over the North Pacific basin with operational flights at Yokota Air Force Base (Japan), Hong Kong, and Guam. An overview of the instrumentation, flight tracks, and collaborating programs is given in an accompanying paper by *Hoell et al.* [this issue]. The purpose of this paper is to provide an overview of the meteorological setting for the PEM-West A mission, including a flight-by-flight discussion of the meteorological factors influencing the transport and chemistry of the trace species observed aboard the DC-8.

¹Lockheed Engineering and Sciences Company, Hampton, VA 23666.

²Massachusetts Institute of Technology, Cambridge, MA 02138.

³Atmospheric Sciences Division, NASA Langley Research Center, Hampton, VA 23681-0001.

⁴University of California, Irvine, CA 92717.

Copyright 1996 by the American Geophysical Union.

Paper number 95JD02799.
0148-0227/96/95JD-02799\$05.00

2. Mean Large-Scale Tropospheric Flow Patterns

The mean large-scale tropospheric flow patterns during PEM-West A can be characterized using 12 hourly gridded meteorological fields obtained from the U.S. National Meteorological Center (NMC) operational analyses. The mean streamline fields, averaged over the entire PEM-West A study period (September 15 to October 22, 1991) are schematically represented at the surface (Figure 1), 850 hPa (~1.5 km, Figure 2), 500 hPa (~5.5 km, Figure 3), and 200 hPa (~12 km, Figure 4).

During PEM-West A the lower-tropospheric flow characterized by the streamline fields at the surface and 850 hPa (Figures 1 and 2) was influenced by large semipermanent anticyclones over the western and eastern North Pacific as well as a less marked anticyclone over China. The cyclonic flow features found over the Philippine Sea and the western equatorial Pacific are not semipermanent but are manifestations of several transient tropical cyclones which often reached their maximum intensities over those areas. Note that at the surface, three regions of converging streamlines define the boundaries among the following principal air streams: (1) continental (Asian) air and marine (western Pacific or South China Sea) air, (2) western and eastern Pacific marine air, and (3) northern hemisphere and southern hemisphere marine air. These three boundaries are also clearly identified by *Newell et al.* [this issue (d)] using the divergent wind components computed from the velocity potential at 1000 hPa.

The mean midtroposphere flow characterized by the 500-hPa winds shown in Figure 3 exhibit two semipermanent subtropical anticyclone centers over southeastern Asia and the western North Pacific. Two north-south oriented trough axes indicated by dashed lines are located just off the east coast of Asia and over the central Pacific. Westerly flow off the Asian continent dominated north of about 25°N. The weak cyclonic center evident over the western equatorial Pacific (near 15°N, 150°E) is again related to the region of intensification and recurvature of tropical cyclones which occur frequently during the fall season (see discussion below). In the upper troposphere (200 hPa, Figure 4) anticyclone centers were again found over southeastern Asia and the western North Pacific, with trough axes off the Asian east coast and over the central

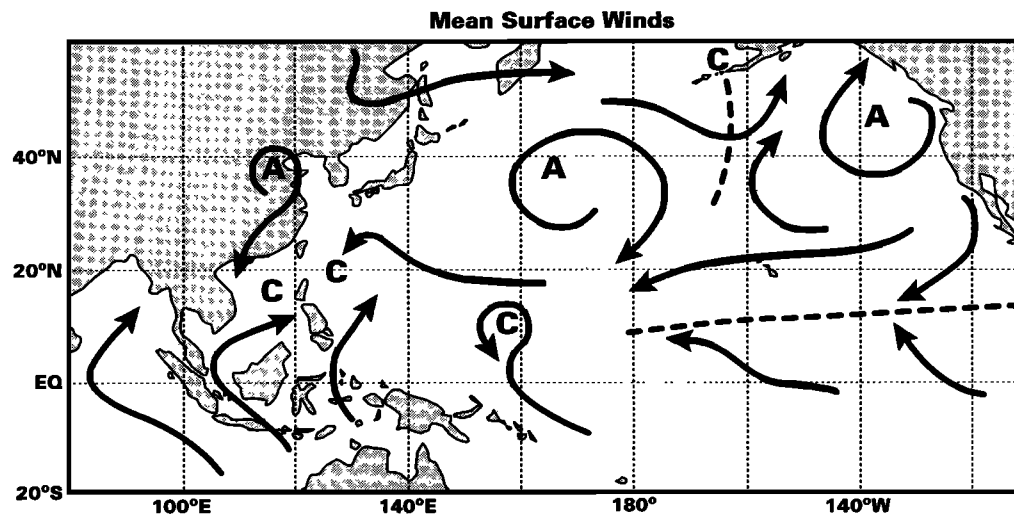


Figure 1. Schematic of the mean surface wind streamline field, derived from 12 hourly (NMC) grid point analyses, averaged over the entire PEM-West A period (September 15 to October 22, 1991). Anticyclonic (A) and cyclonic (C) features of interest are highlighted.

Pacific. Continental flow dominated north of about 25°N, similar to that at 500 hPa.

Several previous studies have been made of the outflow of continental material over the North Pacific. Particularly noteworthy are contributions by Merrill et al. [1989] who discussed meteorological interpretation of surface-measured aerosol material collected from Pacific island stations, and by Prospero et al. [1989] who found that 40-70% of atmospheric nitrate collected at North Pacific island stations originated from continental sources. These data were part of the Sea-Air Exchange Program (SEAREX) which was carried out in 1981-1983. Savoie et al., [this issue] discuss the composition of aerosol samples collected during the PEM-West A experiment at seven Pacific islands stations, including Hong Kong. Merrill [this issue] discusses air parcel trajectories for PEM-West A separately.

Biomass burning annually occurs over parts of western and central Indonesia prior to and during the September-October period. A factor that may have contributed to enhanced biomass burning during PEM-West A was the El Niño/Southern Oscillation (ENSO) event which was under way, which induced an eastward shift of major convection leaving portions of the Indonesia region with below-normal rainfall [Janowiak, 1993]. Media reports indicated that over 70,000 hectares had burned, including 30,000 hectares in southern Borneo alone. This burning produced a massive smoke pall across that region which was often evident on visible GMS satellite imagery (Figure 5). The smoke usually appeared to be thickest between 5°S-5°N and 100°E-115°E and sometimes spread across the Philippines and adjacent areas of the South China Sea. The mean lower-tropospheric flow illustrated in Figures 1 and 2 suggests that some of this persistent smoke could have been trans-

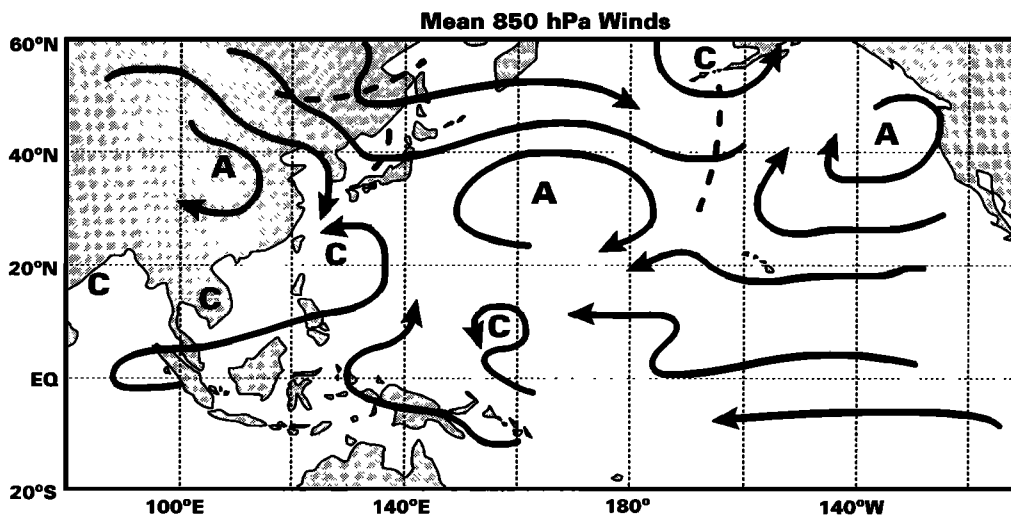


Figure 2. Schematic of the mean 850 hPa wind streamline field, derived from 12 hourly (NMC) grid point analyses, averaged over the entire PEM-West A period (September 15 to October 22, 1991). Anticyclonic (A) and cyclonic (C) features of interest are highlighted.

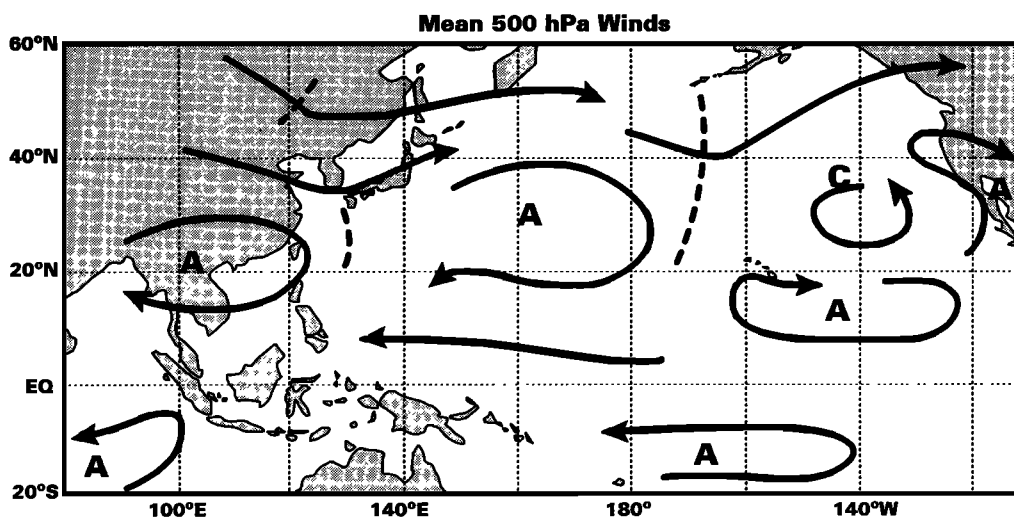


Figure 3. Schematic of the mean 500 hPa wind streamline field, derived from 12 hourly (NMC) grid point analyses, averaged over the entire PEM-West A period (September 15 to October 22, 1991). Anticyclonic (A) and cyclonic (C) features of interest are highlighted.

ported northward and/or northeastward within the boundary layer into portions of the study region. Some evidence of biomass-burning plumes encountered during flight 16 is discussed in section 6.

3. Transient Synoptic Scale Features

In the PEM-West study region, the major transient synoptic scale features affecting long-range transport into and throughout the study area are migratory cyclones and their associated frontal systems and tropical cyclones. During PEM-West A, migratory midlatitude cyclones would frequently form (an average of one per week) and intensify along the east coast of Asia or over the interior of the continent. This coastal area is a region of preferential cyclone formation due to the strong lower-tropospheric temperature gradient in the vicinity of the warm Kuroshio ocean current [Carlson, 1991]. As these cyclones moved across the Pacific, their

trailing cold fronts formed the boundary between continental air of midlatitude (Asian) origin and marine air of either midlatitude or tropical (Pacific) origin. The mean positions of the two primary cold frontal zones (subjectively averaged from an ensemble of 12 hourly NMC frontal analyses) and the southernmost frontal locations are illustrated in Figure 6, together with the mean tracks taken by migratory cyclone and anticyclone centers. Cyclones tended to track eastward and, eventually, poleward as they crossed the Pacific. Anticyclones tended to form over northwestern China, then move eastward or southeastward in the wake of the transient cyclones.

The analysis reported by Gregory *et al.* [this issue] suggests two basic transport pathways of aged marine air into the PEM-West A study area: (1) “north marine” air masses moving eastward, southward, and then westward around the periphery of the Pacific subtropical anticyclone; and (2) “south marine” air masses from the southeasterly trade wind flow or from the southern hemisphere.

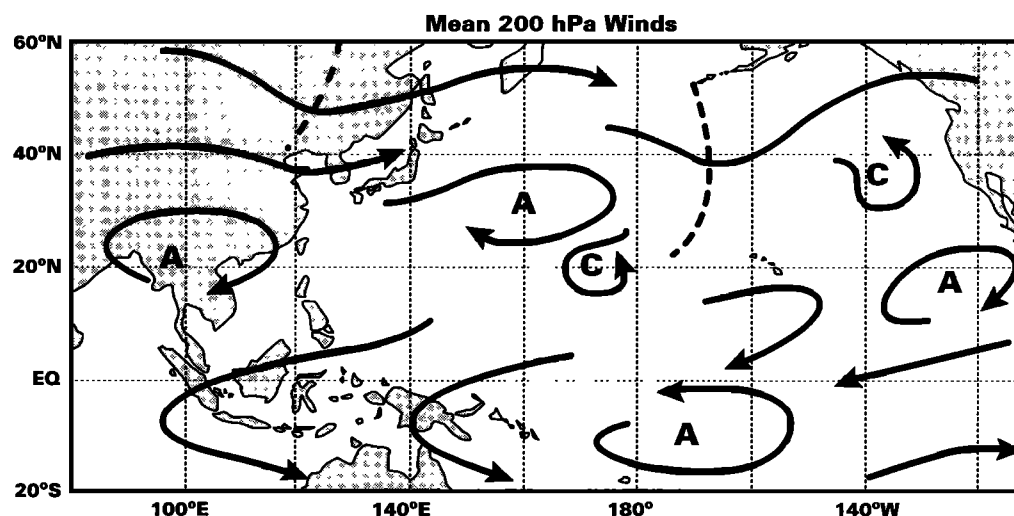


Figure 4. Schematic of the mean 200 hPa wind streamline field, derived from 12 hourly (NMC) grid point analyses, averaged over the entire PEM-West A period (September 15 to October 22, 1991). Anticyclonic (A) and cyclonic (C) features of interest are highlighted.

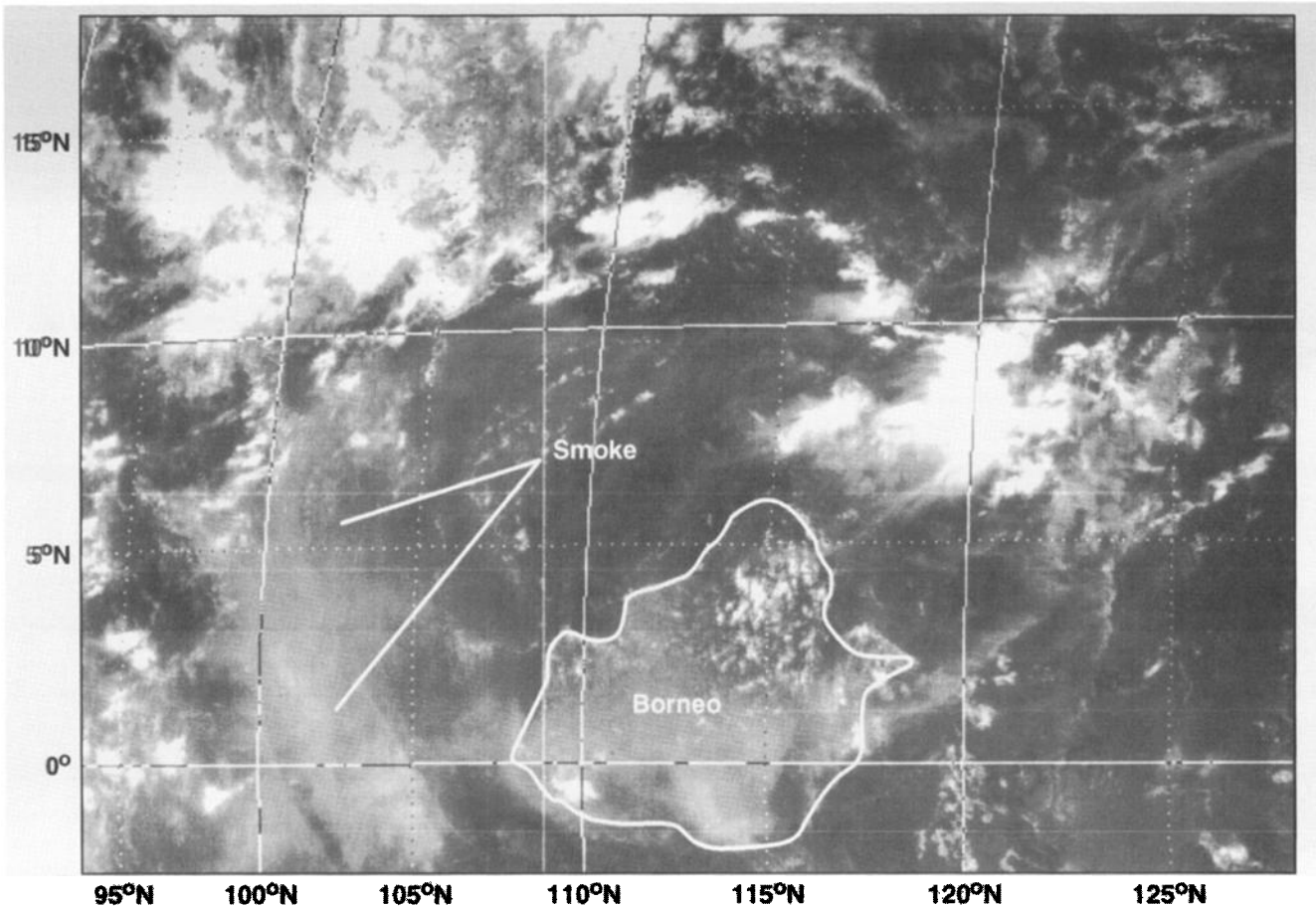


Figure 5. GMS visible sector showing the vast smoke pall (hazy areas) surrounding Borneo on October 8, 1991.

With the Pacific anticyclone and Asian cold front in their mean positions, one would expect a transport of mainly aged North Pacific marine air into the study area. A weaker Pacific anticyclone in tandem with a stronger Asian anticyclone would tend to move the cold front to its southernmost position, bringing continental flow to a larger portion of the sampling region. Tropical cyclones recurring close to the east coast of Asia also induced a stronger continental flow along the western portion of the storm circulation, owing to the increased pressure gradient between the cyclone and the Asian anticyclone which often followed in its wake. *Talbot et al.* [this issue] also stress that at higher altitudes continental outflow can originate much farther upstream than eastern Asia. The reason for this is illustrated in Figure 7a which shows the latitudinal distribution of the polar jet (PJ) and the subtropical jet (STJ) and figure 7b shows a meridional cross section of the mean zonal wind illustrating the higher wind speeds encountered with increasing altitude.

4. Tropical Cyclone Activity

The frequency of tropical cyclones over the western North Pacific and South China Sea normally reaches a peak in August, with September and October being the second and fourth most active months [*Royal Observatory, Hong Kong (ROHK), 1993*]. Climatologically, the September-October period produces 10 tropical cyclones, six of which reach typhoon intensity. September to

October 1991 was a period of near-normal activity with 10 tropical cyclones reported over these two basins with seven reaching typhoon strength. Six tropical cyclones formed during the actual experiment period. One of these (Luke) reached tropical storm strength (maximum sustained wind speeds of at least 17 m s^{-1}), three (Nat, Orchid, and Pat) were classified as typhoons (winds of at least 33 m s^{-1}), and two (Mireille and Ruth) reached “super-typhoon” intensity (winds of at least 67 m s^{-1}). Figure 8 depicts the “best track” paths of these six storms [*Rudolf and Guard, 1992*], and Table 1 lists their dates of formation/dissipation and maximum surface wind speeds.

A three-storm outbreak occurred in mid-September, with storms Luke, Mireille, and Nat. Luke and Mireille recurved north of 20°N , affecting Japan as they accelerated northeastward. The erratic path of Nat was due to the fact that Luke and Mireille effectively eroded the western Pacific subtropical ridge, weakening the steering flow over the South China and Philippine Seas. Orchid and Pat formed on October 1, and their circulations interacted with one another as the storms matured. Ruth did not fully develop until after DC-8 had departed Guam and Wake Island and therefore did not directly affect any of the flights.

One flight was specifically devoted to the sampling of boundary layer inflow and upper tropospheric outflow in the vicinity of a typhoon. Flight 9 investigated Typhoon Mireille southwest of Japan on September 27, sampling the inflow of the southeast quadrant of the circulation and then the outflow at the top of the eye

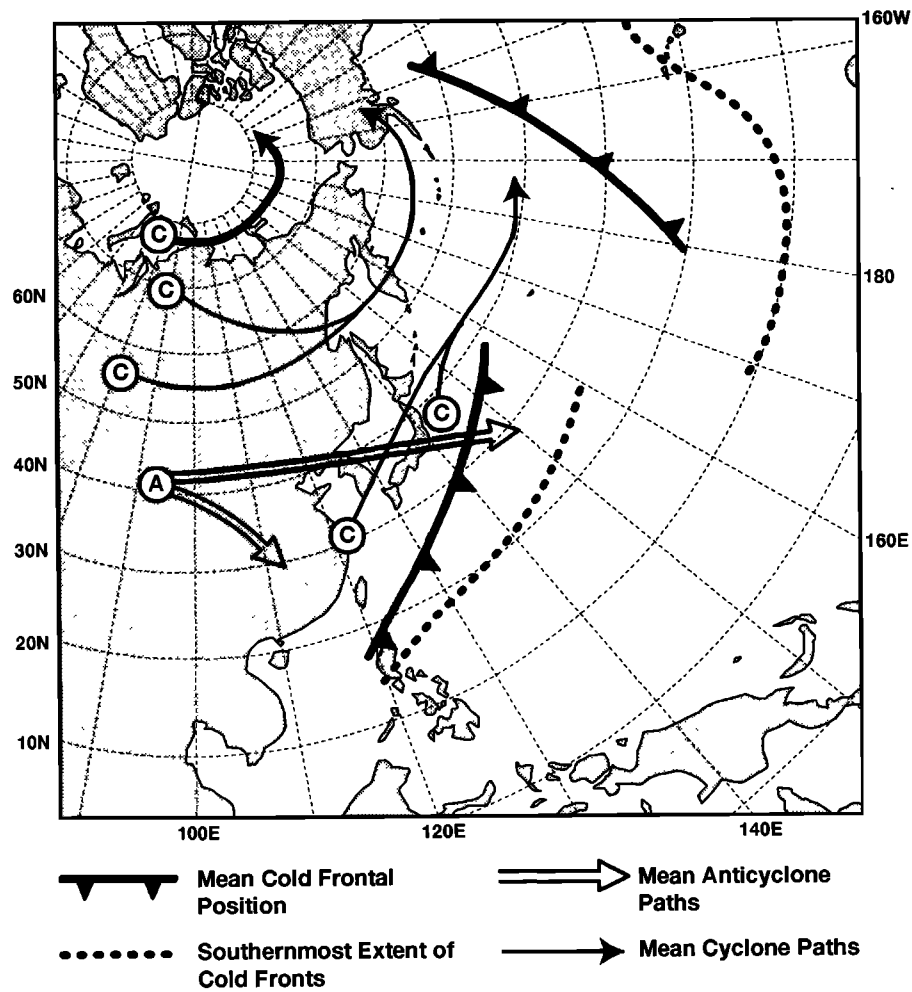


Figure 6. Mean position of the transient midlatitude cold frontal systems (solid cold front symbols) as well as the extreme southward and eastward positions of the fronts (dotted lines) during PEM-West A; mean tracks of migratory cyclones (C) and anticyclones (A) are also depicted.

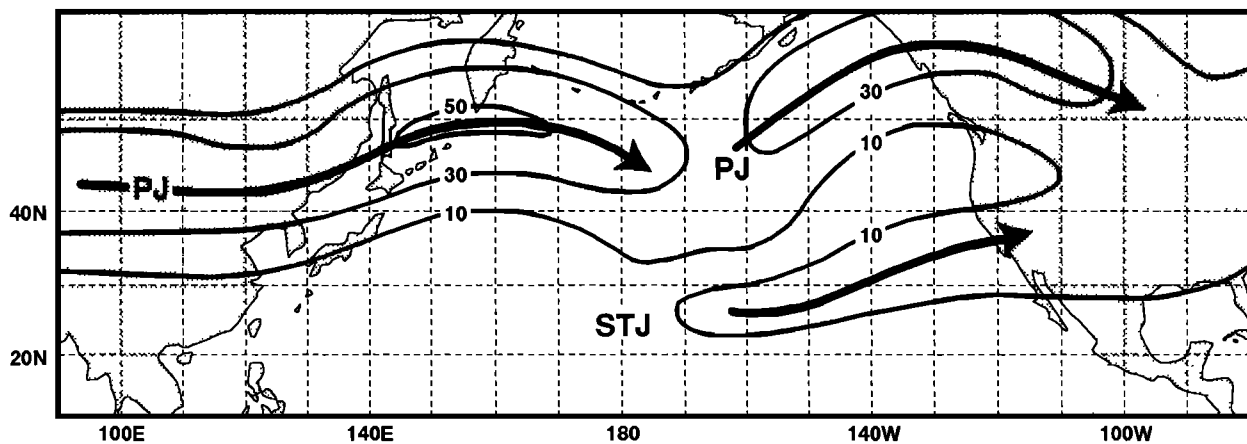


Figure 7(a). Mean NMC 200 hPa wind isotach analysis (m s^{-1}), along with the mean axes of the polar jet (PJ) and subtropical jet (STJ) streams.

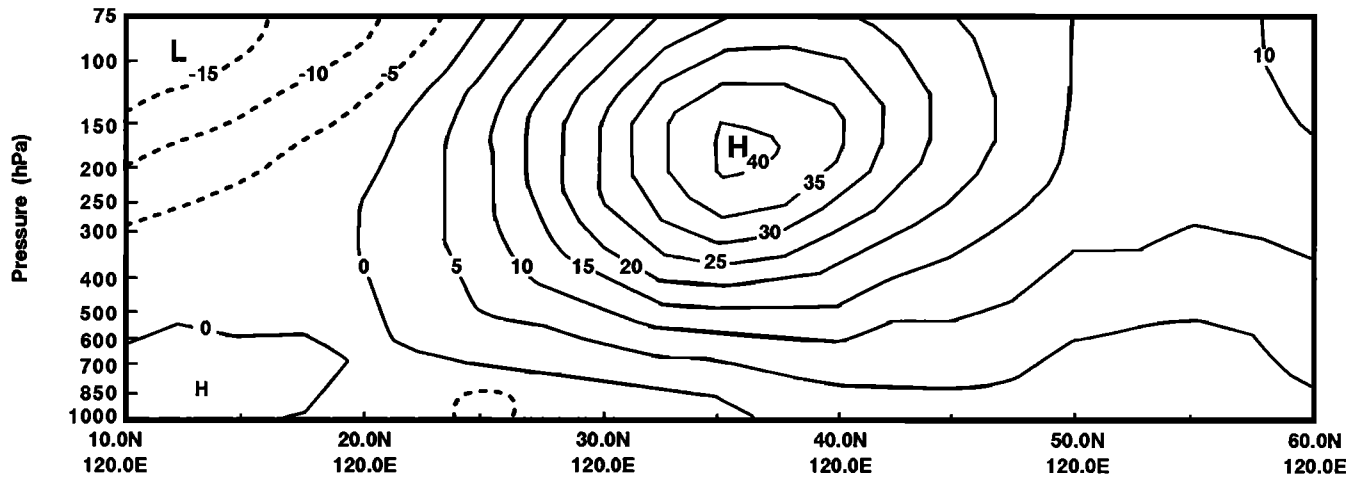


Figure 7(b). Meridional cross section of mean zonal wind (m s^{-1}) for the PEM-West A period, based on (ECMWF) grid point analyses.

region. An in-depth analyses of the transport of trace gases by Mireille is discussed by *Newell et al.* [this issue (a)]. In addition, during the transit flight from Hong Kong to Guam on October 8 (flight 14) the upper levels of the southern quadrant of Typhoon Orchid were sampled.

5. Japan Jet and Stratospheric/Tropospheric Exchange

Figure 7a shows the mean wind isotachs at 200 hPa, along with the locations of the mean axes of the polar and subtropical jet streams. The branch of the polar jet exiting the east coast of Asia (the “Japan jet”) often contained wind speeds of 50 m s^{-1} , occasionally exceeding 80 m s^{-1} . Stratospheric-tropospheric exchange

in the vicinity of such jet streams (near and poleward of the jet axis) is well documented [*Danielsen, 1980; Danielsen and Hipskind, 1980; Bachmeier et al., 1994*], with high ozone mixing ratios and potential vorticity (PV) being classic indicators of air of stratospheric origin.

Over the western North Pacific, significant portions of the troposphere displayed characteristics of stratospherically influenced air, especially at higher latitudes and altitudes. *Browell et al.* [this issue] discuss stratospherically influenced cases observed during PEM-West A flights using the airborne differential absorption lidar (DIAL) aboard the DC-8. On the basis of the DIAL observations, stratospheric air injected into the upper troposphere gradually descends into the middle and lower troposphere and is frequently confined within subsidence inversions which are maintained within the deep semipermanent Pacific subtropical anticyclone. Several specific examples of stratospheric/tropospheric exchange events are discussed in conjunction with the synoptic summaries below.

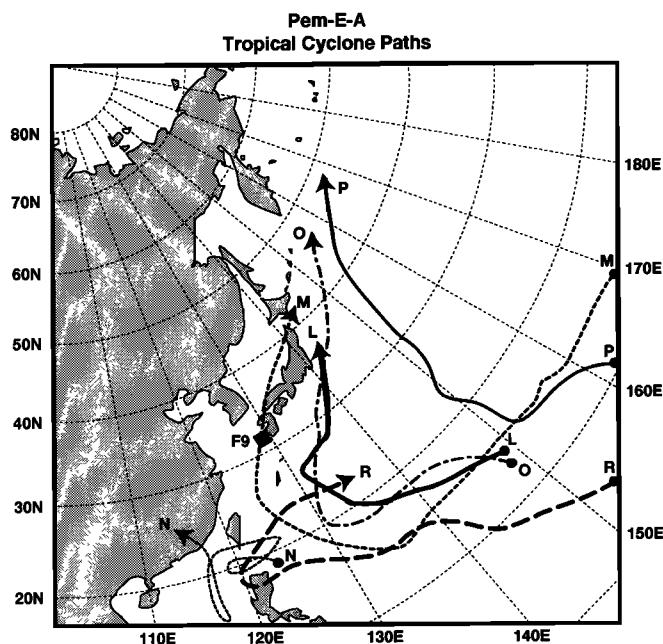


Figure 8. “Best track” paths of tropical cyclones during the PEM-West A period; L, tropical storm Luke; M, supertyphoon Mireille; N, Typhoon Nat; O, Typhoon Orchid; P, Typhoon Pat; R, super-typhoon Ruth. The square (labeled F9) denoted where Mireille was intercepted during flight 9 (based on data from *Rudolf and Guard, [1992]*).

6. Flight-by-Flight Synoptic Summaries

The PEM-West A mission consisted of 21 flights. The first three were test flights; the remaining 18 consisted of eight survey or transit flights, four local flights from Yokota Air Force Base in Japan, two local flights from Hong Kong, three local flights from Guam, and one local flight from Hawaii. This section will provide a synoptic summary for each flight beginning with flight 4. For selected flights, examples are included of the relationship between the chemical measurements and the meteorological features.

Flight 4; September 16, 1991 (1704-2251 UT)

Flight 4 was the initial survey flight from Moffett Field, California to Anchorage, Alaska. In the lower troposphere a high-pressure system dominated western North America and adjacent portions of the eastern North Pacific. An extensive area of low pressure covered the Aleutians and Alaska peninsula region, with an associated frontal boundary stretching from the Gulf of Alaska southwestward toward the Hawaiian Islands. In the middle to upper troposphere a strong ridge was centered along the northern California coast, with the ridge axis running northward into western Canada and the Oaken Territory. A broad upper trough of low pressure was located over the North Pacific, with closed low cen-

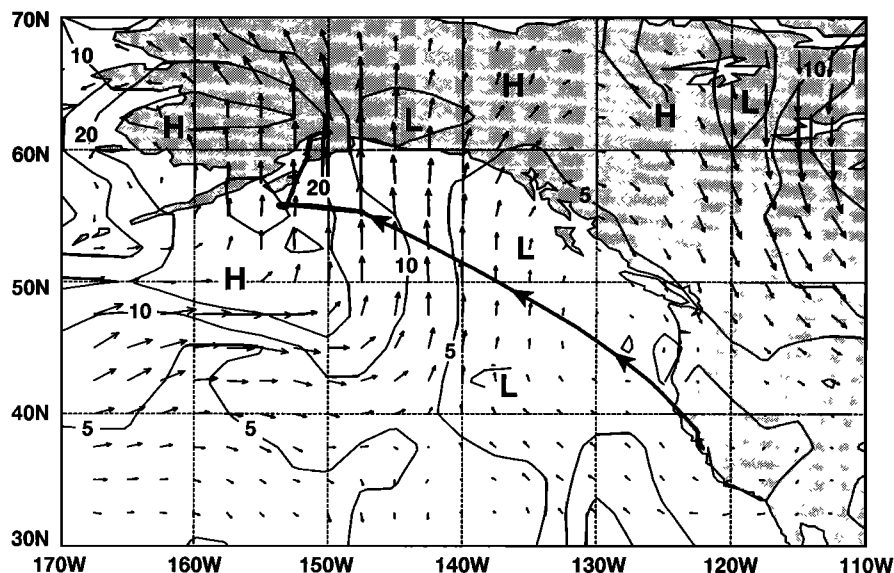


Figure 9. Potential vorticity ($10^{-7} \text{ K m}^2 \text{ kg}^{-1} \text{ s}^{-1}$) and wind vectors (m s^{-1}) for 0000 UT, September 17, 1991, based on ECMWF data. Thick solid line represents DC-8 track. Stratospheric air was entered near 56°N , 148°W .

ters over the eastern Bering Sea and near the Kamchatka peninsula. These features were quite similar to the mean flow patterns shown in Figures 1-4. The axis of the polar jet stream at 300 hPa was located along 40° - 45°N across the western and central North Pacific. The jet then turned sharply northward over the Gulf of Alaska. High values of potential vorticity at 400 hPa ($\sim 6 \text{ km}$) suggested that stratospheric air was present at flight level over southwestern Alaska. A map of this high potential vorticity region, based on ECMWF data on the 315 K surface, is shown in Figure 9 along with the flight track. Note that the DC-8 flight track turned westward at about 55°N , 146°W into the high potential vorticity region. The DC-8 flew for about 25 min at about 11.3 km in the stratospheric air then started a gradual descent at about 2120 UT, reaching about 400 m at 2147 UT. A time series of SO_2 , CO , CH_4 , O_3 , and flight altitude is shown in Figure 10. The elevated O_3 and reduced CO and CH_4 are clear indicators of stratospheric air. Note that elevated concentrations of SO_2 were also observed during this encounter with stratospheric air. Analysis by Thornton *et al.* [this issue] attributed this to the June 1991 eruption of Mount Pinatubo, which injected huge quantities of sulfur into the stratosphere.

Extensive low-level clouds (stratus, stratocumulus) were evident along coastal California and the surrounding eastern North Pacific. A small patch of middle- and high-level clouds (altocumulus, cirrus) was located just off the northern California coast. A band of layered cloudiness associated with the frontal boundary covered much of the Gulf of Alaska. Otherwise, no significant cloud features were apparent along the flight region.

Flight 5; September 17-18, 1991 (1857-0328 UT)

Flight 5 was the second leg of the survey flight from Moffett Field, California, to Yokota AFB, Japan, via Anchorage, Alaska. The Aleutian surface low was weakening over the Bering Sea, while another low was moving eastward from the Kamchatka peninsula. High pressure dominated from the east coast of Japan across the western North Pacific. A quasi-stationary frontal boundary was oriented west to east just to the south of Japan between 30° and 35°N , separating a drier modified continental air mass to the north from a moist marine air mass to the south. Tropical

storm Luke was centered at 25.5°N , 130.7°E at 0000 UT on September 18 and was moving slowly northward (Figure 11). A broad trough of low pressure at 500 hPa remained across the North Pacific, as the individual lows centered over the Kamchatka peninsula and the Bering Sea weakened and began to fill. A strong westerly flow off the Asian continent dominated over the North Pacific in the 35° - 50°N latitude belt. The axis of the polar jet stream at 300 hPa was oriented west to east along about 38°N across the western and central North Pacific. Over the eastern North Pacific the jet turned northeasterly toward the Gulf of Alaska.

Patchy low- and middle-level clouds (stratocumulus, altocumulus, altostratus) were evident across much of the Bering Sea and in the vicinity of the Kamchatka low. High pressure off the east coast of Japan kept that region generally clear. Extensive layered cloudiness associated with tropical storm Luke covered much of southern Japan.

During this flight and on flights 9 and 14, dimethyl sulfide (DMS) mixing ratios were observed in the free troposphere (115 pounds per trillion volume (pptv)) comparable to those observed in the boundary layer ($\sim 160 \text{ pptv}$). The free troposphere measurement was made at 2100 UT at 54°N , 171°W , and an altitude of 8 km, between the Kamchatka and Bering Sea low-pressure areas ("FT" in Figure 11). The boundary layer measurement was obtained at 2230 UT, near 53°N , 174°E at an altitude of 365 m ("BL" in Figure 11). The aircraft down-looking video showed convective clouds reaching almost up to the aircraft flight level, suggesting a mechanism for the vertical transport of boundary layer air to the 8 km altitude. The other two occasions where this event occurred were in Typhoons Mireille (e.g., flight 9) [see Newell *et al.*, this issue (a), Table 3] and Orchid (flight 14, noted below), where there was also opportunity for rapid vertical mixing.

Flight 6; September 22, 1991 (0224-0947 UT)

Flight 6 was a local flight from Yokota Air Force Base (AFB). The flight profile consisted of flights at several different altitudes in the same vertical plane. Such a profile is characterized here as a "wall profile."

After tropical storm Luke moved northeastward across Japan on

TIME SERIES OF SO₂, CO, CH₄, O₃, & HEIGHT
MISSION 04, 16 SEP., 1991

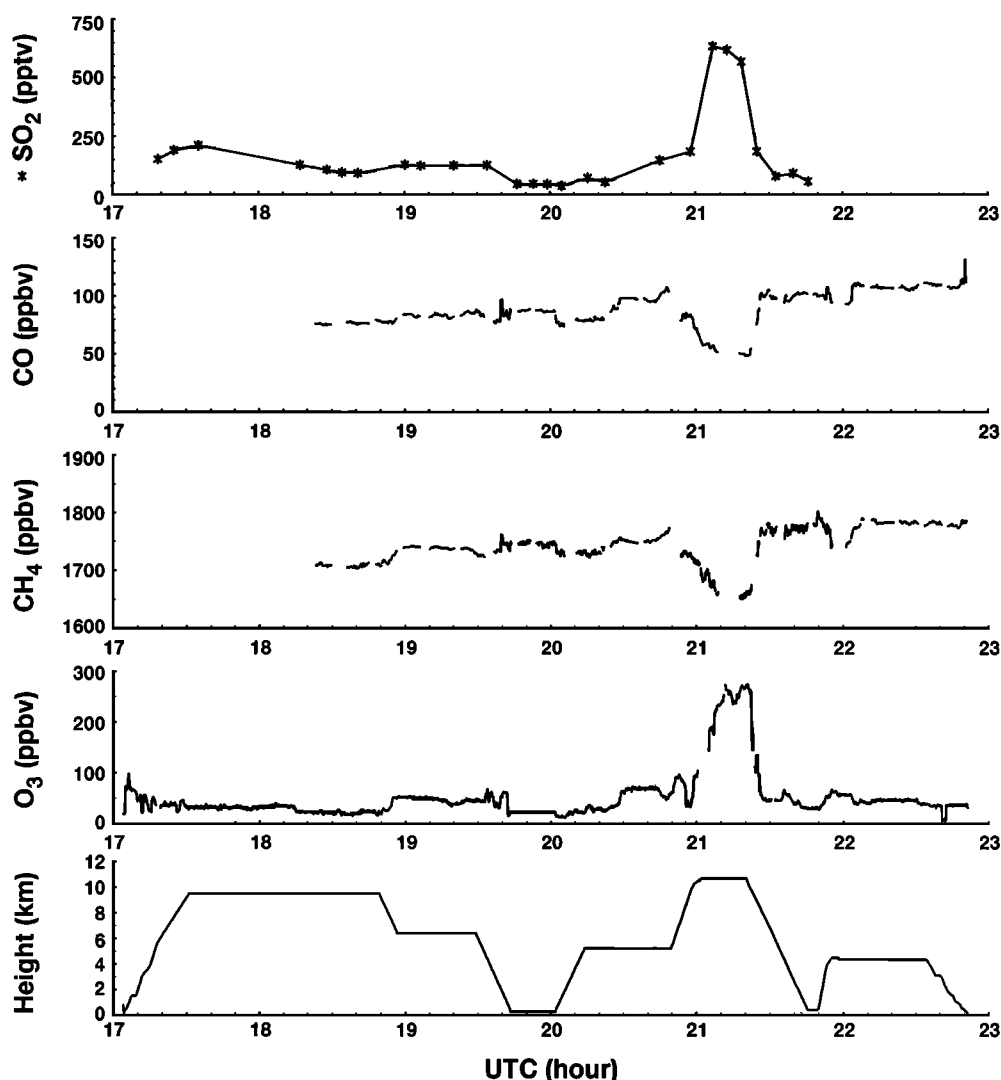


Figure 10. Times series of SO₂ (pptv), CO (ppbv), CH₄, O₃ (ppbv) and DC-8 altitude (km) for mission 4 on September 16, 1991.

September 19, a cyclone moved from Manchuria and Korea eastward over the northern Sea of Japan. A cold front trailing from this cyclone stretched from just east of Japan southwestward toward Taiwan. This frontal boundary was the leading edge of a weak surge of continental air from northern China. The southward progress of the cold front was hindered by the presence of Typhoons Nat (21.6°N, 124.1°E) and Mireille (15.5°N, 134.5°E) over the Philippine Sea (see Figure 12a at 1000 hPa). The frontal cloud band was positioned just to the south and east of Japan, but cloudiness was less extensive in the region under the subtropical ridge axis (south of 25°-30°N).

The subtropical ridge aloft had been intensifying to the south of Japan following the exit of tropical storm Luke. The ridge axis was situated between 20° and 30°N (see Figure 13a at 300 hPa) from southern China eastnortheastward across the North Pacific. A westerly flow off the Asian continent prevailed to the north of the ridge axis, while a south-southeasterly flow was present over the flight region south of the ridge axis. The axis of the polar jet stream

at 300 hPa was located between 35° and 40° across China, then turned northeastward across Japan. The jet was most intensive over the central North Pacific, with wind speeds in excess of 70 m per second.

Flight 7; September 24, 1991 (0211-0915 UT)

Flight 7 was configured as a wall profile, east and northeast of Yokota AFB. A weak cyclone was located off the southern tip of the Kamchatka peninsula, with an associated cold front stretching southwestward. Behind the cold front an anticyclone had spread from the Sea of Japan eastward across Japan and over the adjacent waters of the western North Pacific. This frontal boundary was still defining the leading edge of the weak surge of continental air from northern China. Typhoon Mireille was located at 20.3°N, 128.9°E at 1200 UT on September 24 (Figure 12b). The Pacific subtropical ridge axis aloft was along 30°N (Figure 13b) with a strong westerly flow off the Asian continent evident north of about 35°N. The

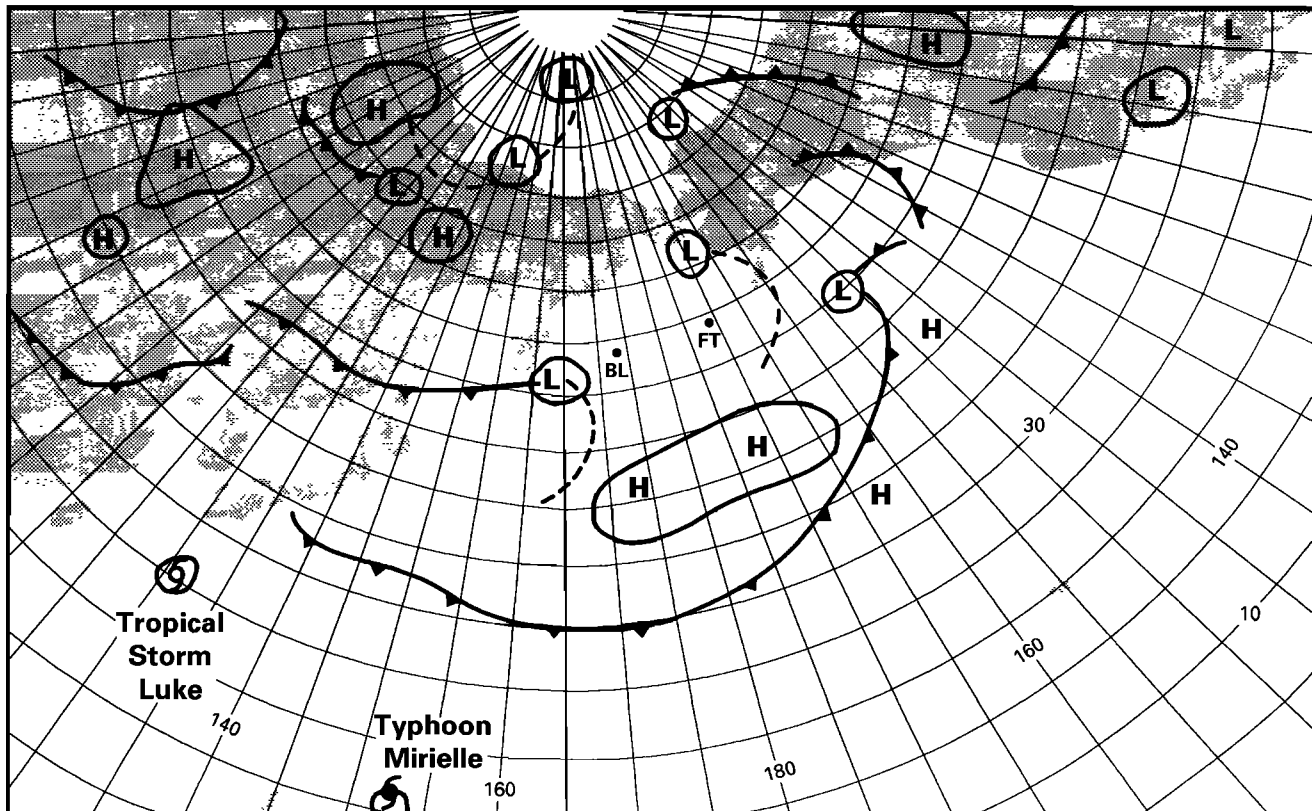


Figure 11. Schematic NMC surface analysis for 0000 UT, September 18, 1991. High- (H) and low-pressure (L) centers are denoted, along with cold fronts and trough lines (standard symbols). FT and BL are positions of (DMS) samples in the free troposphere and boundary layer, respectively, as discussed in text.

intensity and aerial coverage of the Pacific subtropical ridge had been weakening during the past several days, especially along the western periphery, with the approach of Typhoon Mirielle. The axis of the polar jet stream at 300 hPa was located between 35° and 40°N across China, Korea, and Japan, then turned northeastward over the western Pacific. Middle- and high-level clouds (altocumulus, altostratus, cirrus) covered southern Japan, but the flight region to the east and northeast was generally clear.

The wall profile was made along 147°E, nearly perpendicular to the flow along the 320K surface shown in Figure 14. A region of high potential vorticity was intercepted near 36°N, and a cross section (Plate 1) shows a direct connection with the stratosphere. In situ ozone values near 100 pounds per billion volume (ppbv) were measured at about 9 km, and the upper tropospheric ozone measured by the airborne DIAL [see *Browell et al.*, this issue, Plate 3] was likewise high.

Flight 8; September 25-26, 1991 (1656-0017 UT)

Flight 8 occurred southeast of Yokota during a night-to-day transition. Another weak cold front had pushed from Mongolia and Manchuria southeastward across Japan. The trailing edge of this frontal boundary was oriented west to east at around 32°-33°N, just south of Japan. An anticyclone which followed the front was positioned along the east coast of Japan (Figure 12c).

The Pacific subtropical ridge was intensifying, with the ridge axis still just to the south of 30°N over the flight region (Figure 13c). Typhoon Mirielle was beginning to penetrate the western periphery of the ridge as it recurved and moved northward. A

strong westerly flow off the Asian continent was still evident north of about 35°N. The axis of the polar jet stream at 300 hPa stretched from 36°N over China to 40°-45°N northeast of Japan. Layered cloudiness associated with the front covered much of Japan. South of 30°N, the region under the subtropical ridge axis was generally clear.

Flight 9; September 27, 1991 (0105-0739 UT)

Flight 9 was specifically designed to study trace gas transport associated with Typhoon Mirielle. A large anticyclone was situated east of Japan (Figure 12d). Typhoon Mirielle was over the East China Sea (29.8°N, 127.6°E at 0000 UT, September 27) and was accelerating rapidly toward the northeast. With the approach of Mirielle the trailing edge of the old cold frontal boundary (which had become stationary to the south of Japan) was pushed northward across Japan, bringing a maritime tropical air mass to all but the northern half of Japan.

The subtropical ridge had amplified slightly and built northward just to the east of Japan (Figure 13d). In the midtroposphere the deep cyclonic circulation associated with Typhoon Mirielle was just southwest of Japan. The eye and extensive spiral bands and cirrus outflow of Typhoon Mirielle were very prominent and covered much of Japan, the Sea of Japan, and the Yellow Sea. From satellite animation the best outflow aloft appeared to be from the northwestern quadrant, although outflow from the southeastern quadrant was also well defined. A satellite image and a discussion of the trace constituents for this case and their interpretation is given by *Newell et al.* [this issue (a)].

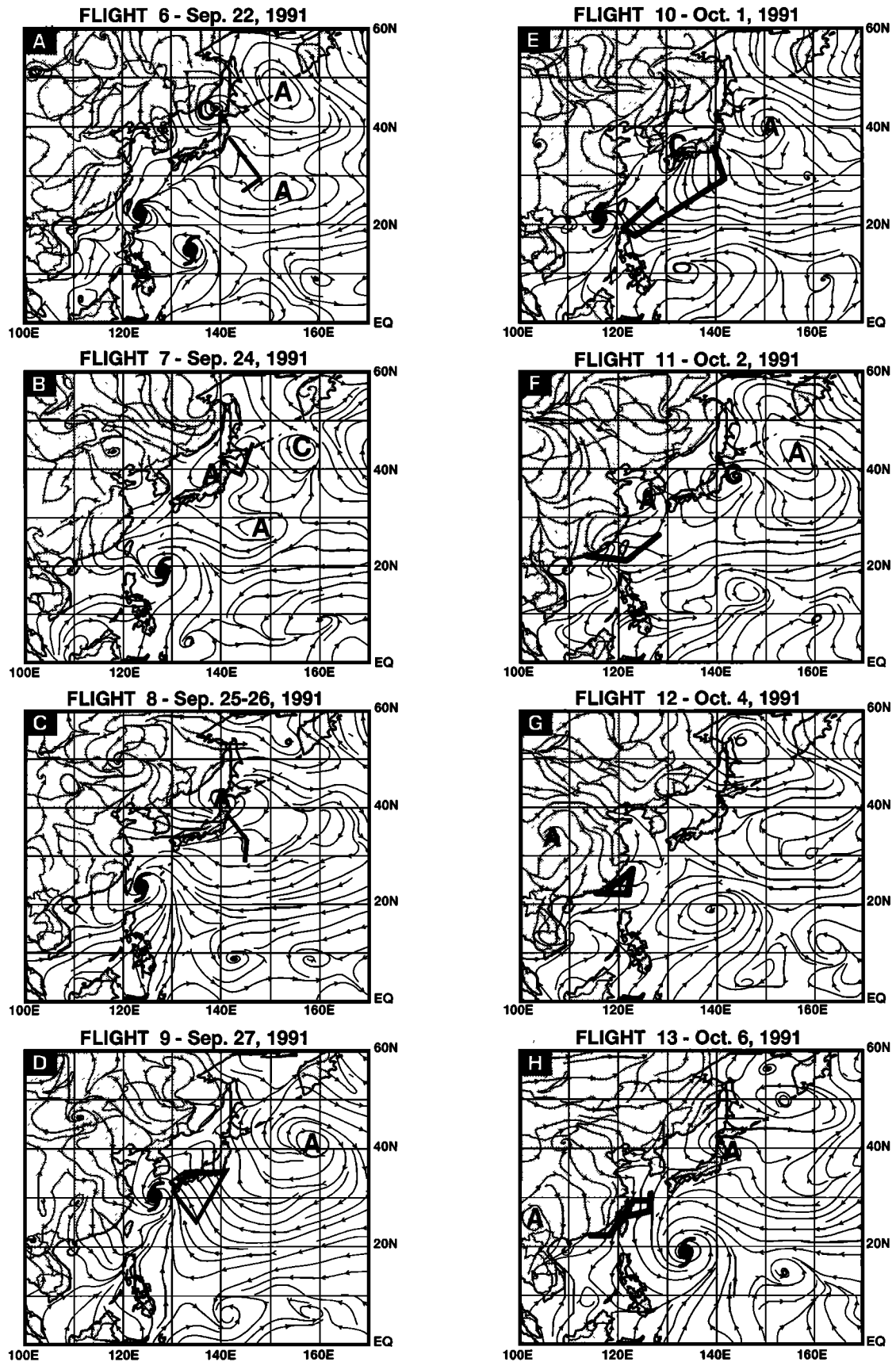


Figure 12. Streamlines for flights 6-21, drawn from NMC analyses at 1000 hPa. Anticyclone (A) and cyclone (C) centers of interest are highlighted. Tropical cyclone centers are denoted by the standard symbol. Flight track is indicated by a thick solid line.

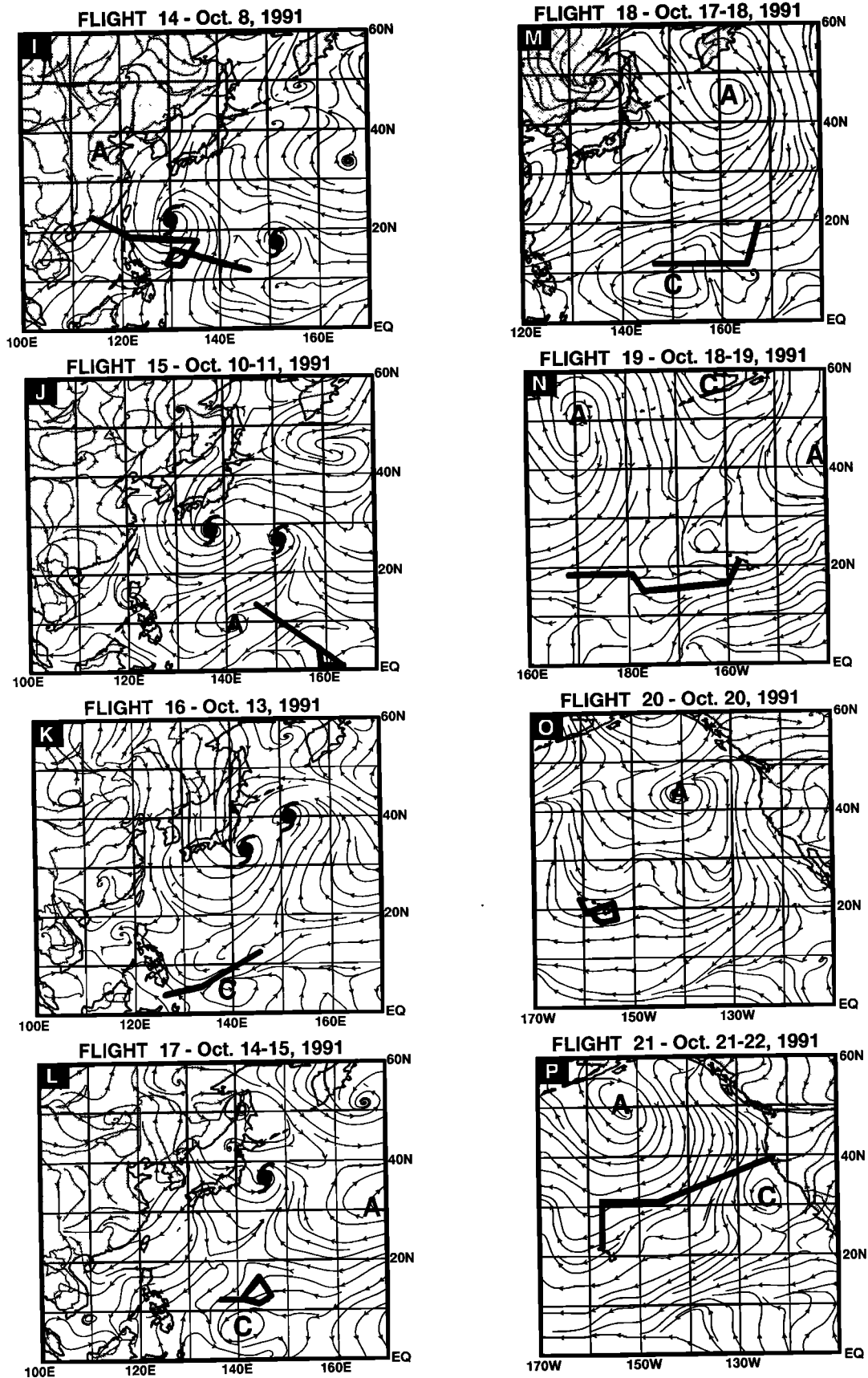


Figure 12. (continued)

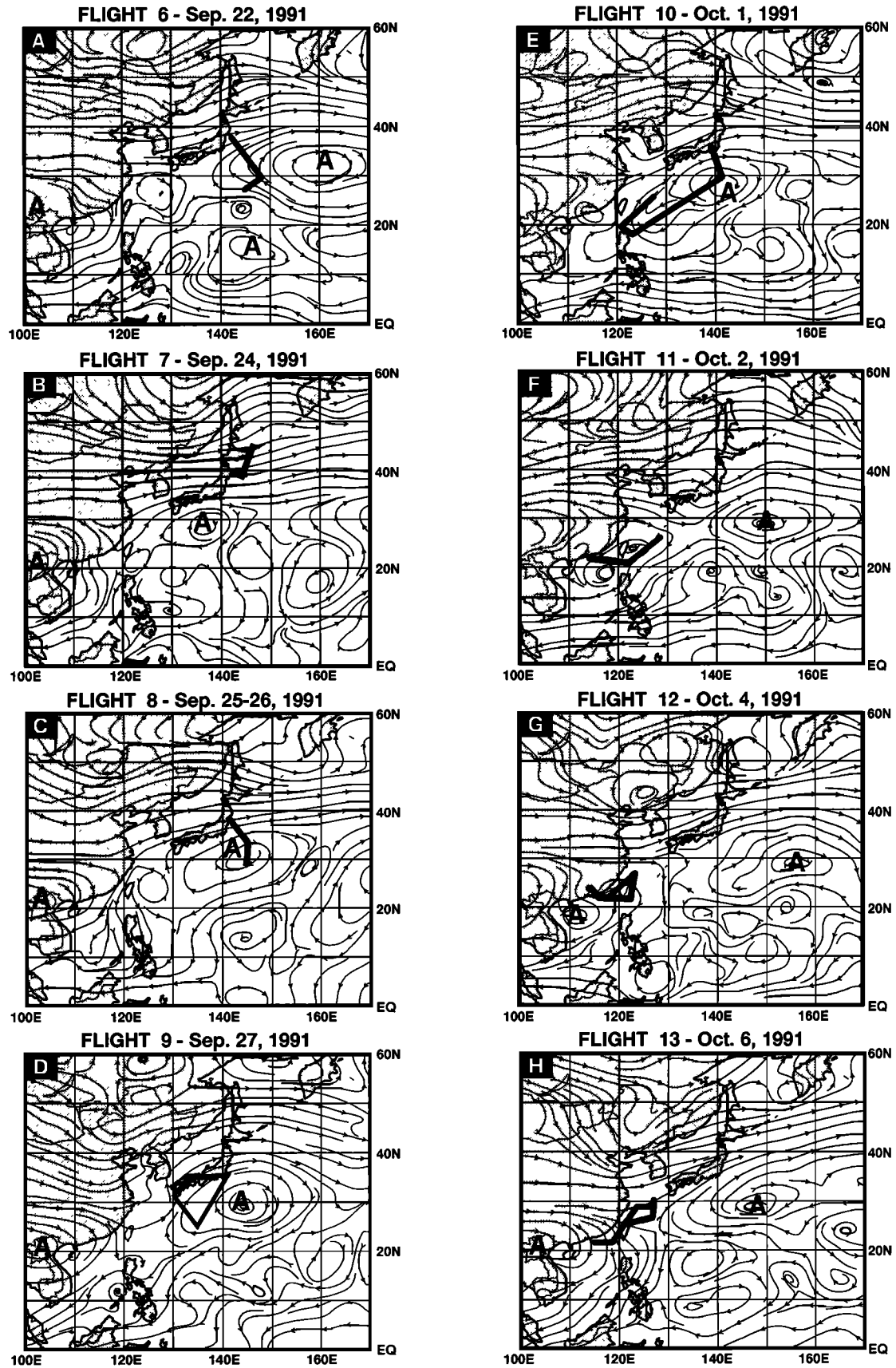


Figure 13. Streamlines for flights 6-21, drawn from NMC analyses at 300 hPa. Anticyclone (A) and cyclone (C) centers of interest are highlighted. Tropical cyclone centers are denoted by the standard symbol. Flight track is indicated by a thick solid line.

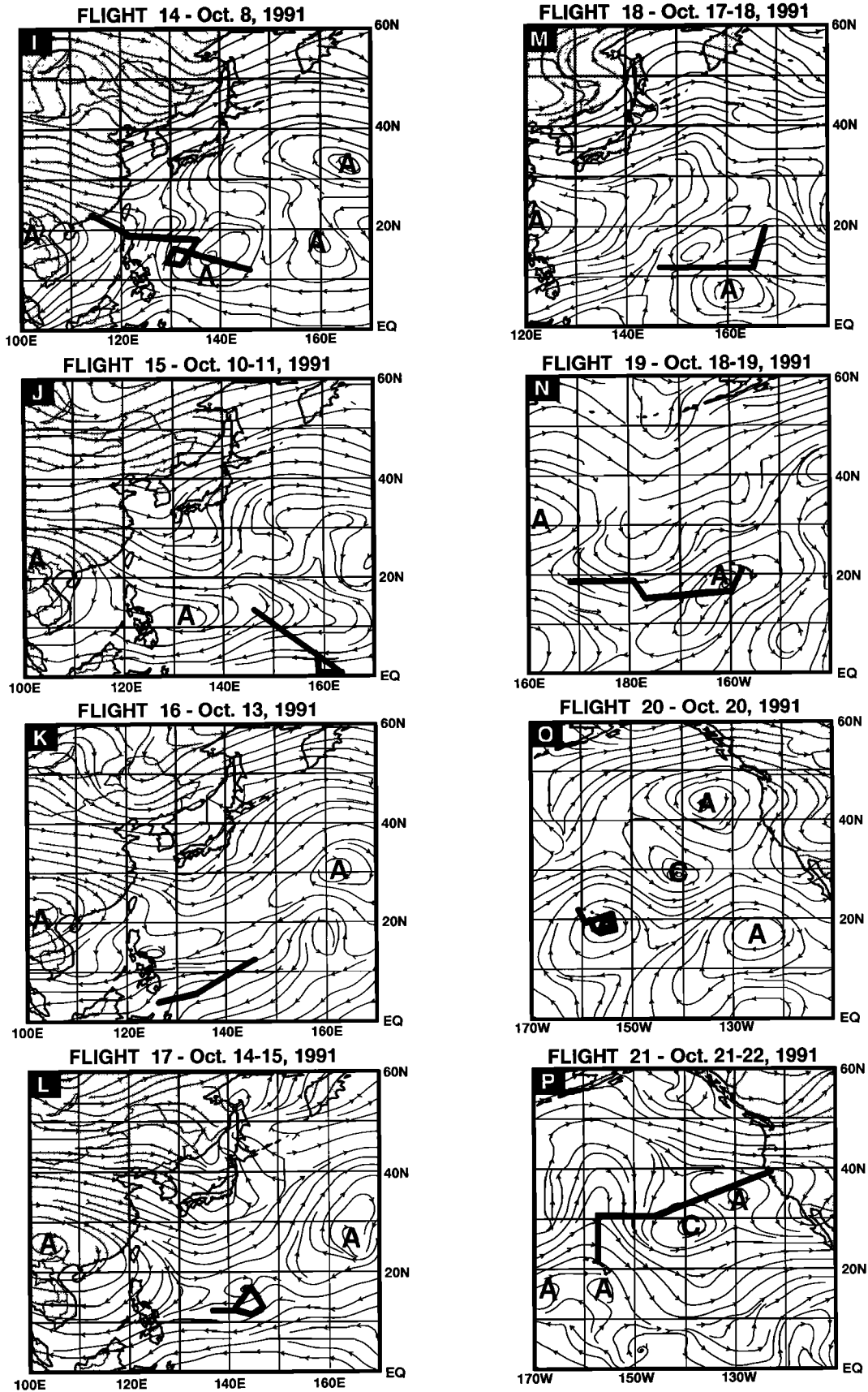


Figure 13. (continued)

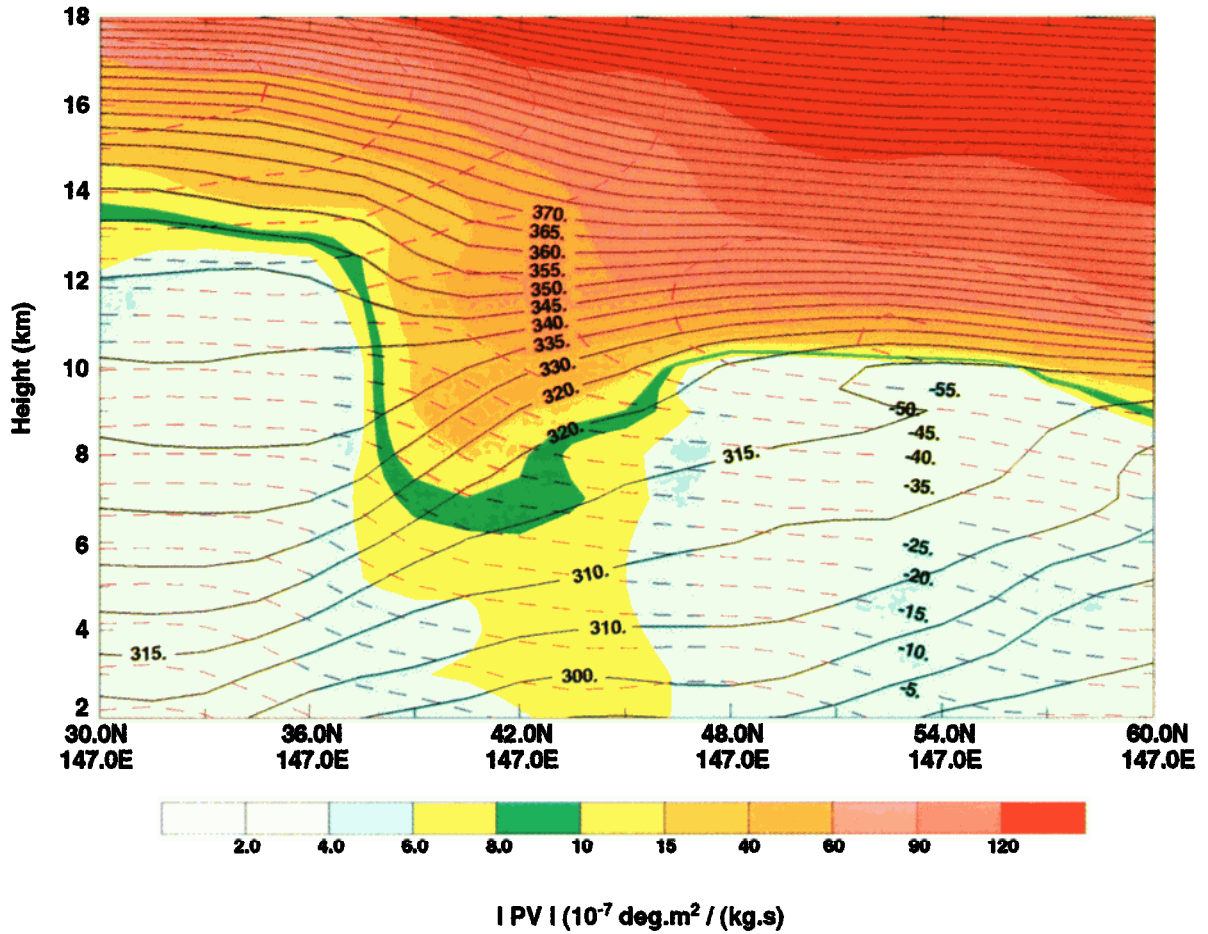


Plate 1. Meridional cross section of potential vorticity ($10^{-7} \text{ K m}^2 \text{ kg}^{-1} \text{ s}^{-1}$) from ECMWF analysis data at 0000 UT, September 24, 1991. Solid line is potential temperature ($^{\circ}\text{K}$), dashed line is temperature ($^{\circ}\text{C}$).

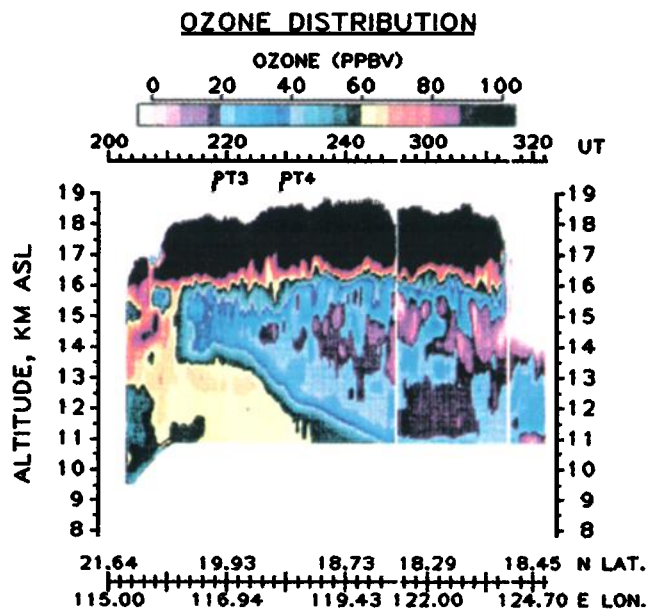


Plate 2. Cross section of ozone mixing ratio (ppbv) from (DIAL) during flight 14 on October 8, 1991.

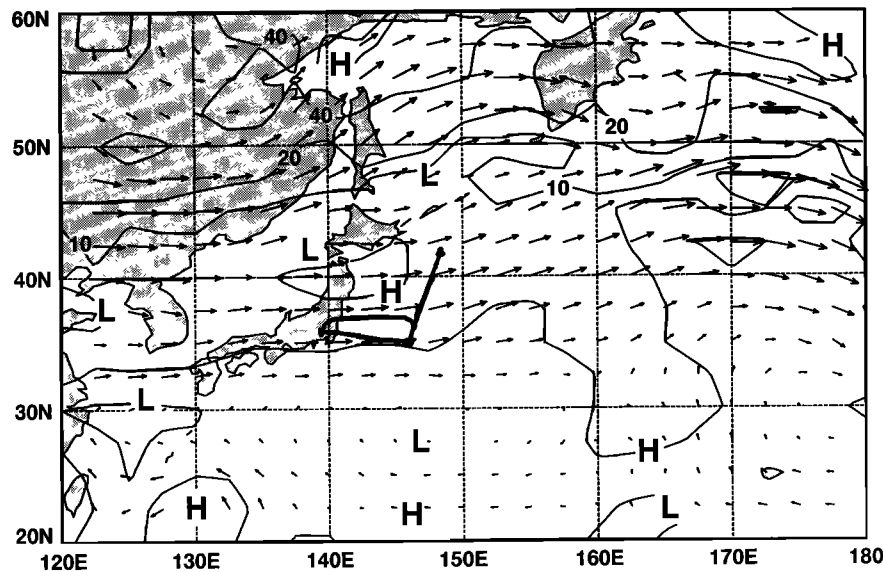


Figure 14. Potential vorticity ($10^{-7} \text{ K m}^2 \text{ kg}^{-1} \text{ s}^{-1}$) and wind vectors (m s^{-1}) on the 320 K surface from ECMWF analysis data at 0000 UT, September 24, 1991. Thick solid line represents the DC-8 flight track.

Flight 10; October 1, 1991 (0244-0935 UT)

Flight 10 was the first leg of the transit/survey flight from Yokota AFB to Hong Kong, via Okinawa, Japan. An anticyclone had moved eastward from northern China across Korea and the Sea of Japan and was situated east of Japan. A cyclone which developed near Taiwan had moved northeastward and was located over southwestern Japan. Severe tropical storm Nat was tracking slowly northward across the South China Sea (Figure 12e).

The subtropical ridge had become well established across the western North Pacific between 20° and 30°N . The cyclonic circulation of Nat was evident even at 300 hPa just off the South China Coast (Figure 13e). A weak short-wave trough of low pressure was propagating eastnortheastward from central China across the Yellow Sea and over the Sea of Japan. A very localized 30 m s^{-1} jet streak was associated with this wave.

A central dense overcast obscured the eye of Nat, which was just off the South China Coast between Hong Kong and the southern tip of Taiwan (Figure 15). Outflow aloft from the northern quadrant of Nat was being drawn north-northeastward into the short-wave trough over the East China Sea. A well-organized area of convection had formed just east of Taiwan, aided by strong upper level diffluence over that region.

On the southbound leg from Yokota, DIAL recorded a layer of elevated ozone between 4.5 and 7 km extending over at least 600 km along the flight track (26° - 31°N , 141° - 137°E). It was associated with potential vorticity values of $4\text{-}6 \times 10^{-7} \text{ K m}^2 \text{ kg}^{-1} \text{ s}^{-1}$ within the 320-330 K potential temperature layer (Figure 16). The winds shown in Figure 16 indicate that the flow within this layer was from the southwest.

Flight 11; October 2, 1991 (0002-0222 UT)

Flight 11 was the second leg of the transit/survey flight from Yokota AFB to Hong Kong via Okinawa, Japan. A cyclone had moved northeastward across southern Japan and was located just off the east coast of Japan. A cold front trailed southwestward from this cyclone toward northern Taiwan. An anticyclone behind the front was situated over the Yellow Sea and the East China Sea. Tropical storm Nat had made landfall along the South China Coast

and was weakening rapidly as it moved northeastward (Figure 12f). Satellite imagery loops indicated a low-level offshore flow of continental air along the South China Coast west of Nat. Aloft, the subtropical ridge was still prominent across the western North Pacific between 20° and 30°N . However, the western periphery of the ridge was weakening as tropical storm Nat moved inland across the South China Coast (Figure 13f).

Cloudiness associated with the remnants of tropical storm Nat covered much of southeast China and adjacent portions of the Taiwan Strait. In addition, clouds remaining from the previous days' convective cluster east of Taiwan had drifted northeastward over the East China Sea. New convection developed during the day off the southern tip of Taiwan.

Flight 12; October 4, 1991 (0151-1015 UT)

Flight 12 was a local flight from Hong Kong which included a wall profile east of Taiwan. A large anticyclone had been building over north central China and was beginning to move southeastward. The leading edge of this surge of continental air had moved off the southern and eastern China coasts and was passing southeastward across the island of Taiwan (Figure 12g). The main portion of the subtropical ridge aloft had moved eastward to the central North Pacific. A weak off-continent flow existed at high altitudes along much of the southern and eastern China coasts (Figure 13g).

Cloudiness associated with the remnants of tropical storm Nat had drifted slowly northeastward and was moving into the East China Sea and the northern Taiwan Strait. Embedded thunderstorms were evident along the eastern China coast. Scattered patches of low- and middle-level clouds (cumulus, stratocumulus, altocumulus) covered the South China Sea and the southern end of the Taiwan Strait. A multilevel wall profile, in which flights are made at several altitudes along the same track, was flown just to the east of Taiwan.

Flight 13; October 6, 1991 (0119-0815 UT)

Flight 13 was an intensive flight northeast of Hong Kong. A large anticyclone was centered over central China. Tropical storm

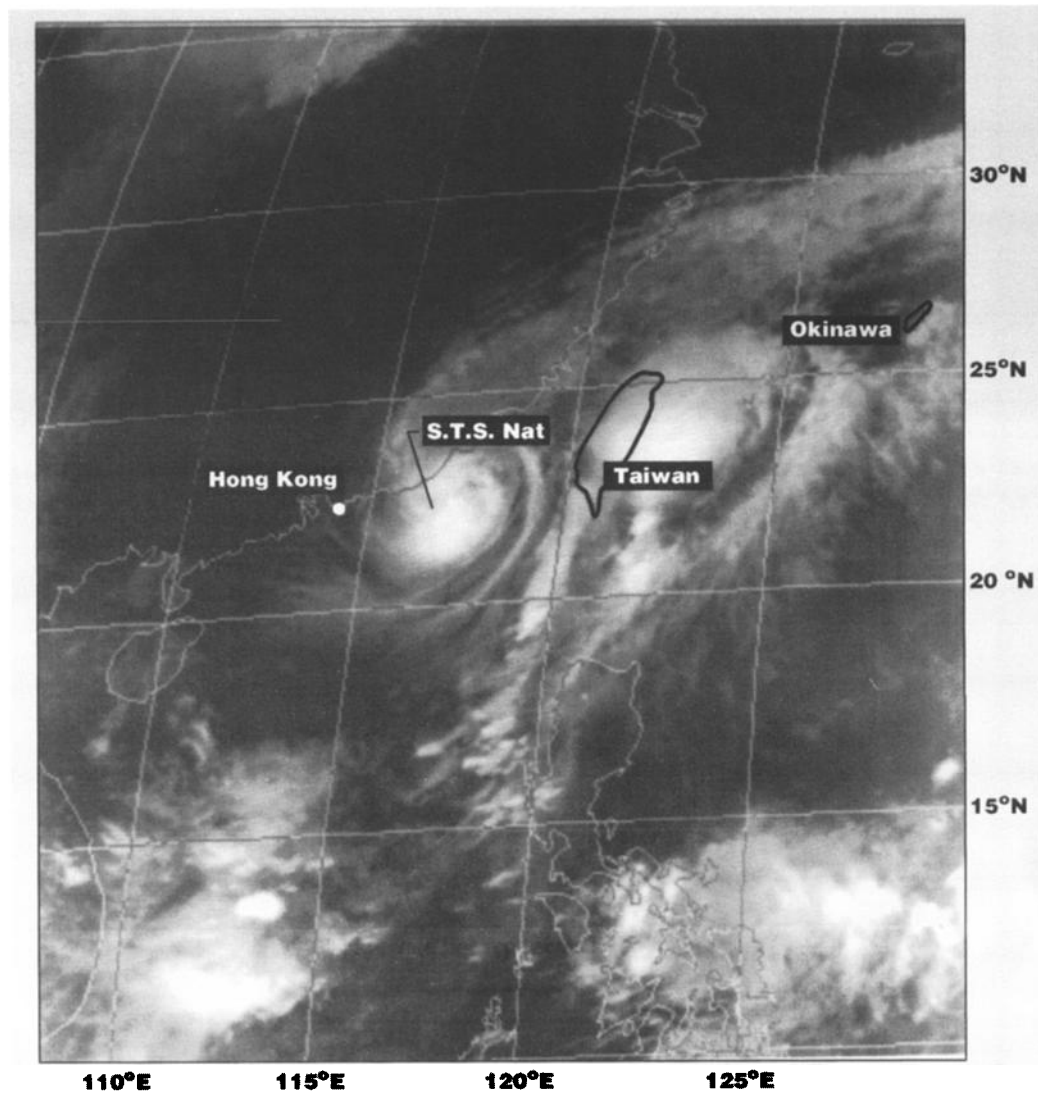


Figure 15. GMS infrared satellite image for 0532 UT, October 1, 1991.

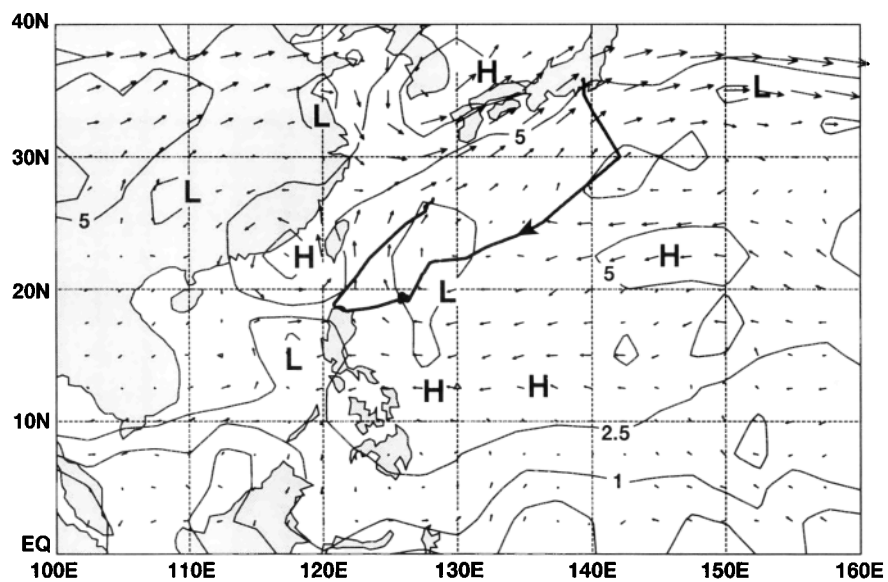


Figure 16. Potential vorticity ($10^{-7} \text{ K m}^2 \text{ kg}^{-1} \text{ s}^{-1}$) and wind vectors (m s^{-1}) on the 325 K surface from ECMWF analysis data at 0000 UT, October 1, 1991. Thick solid line represents DC-8 flight track.

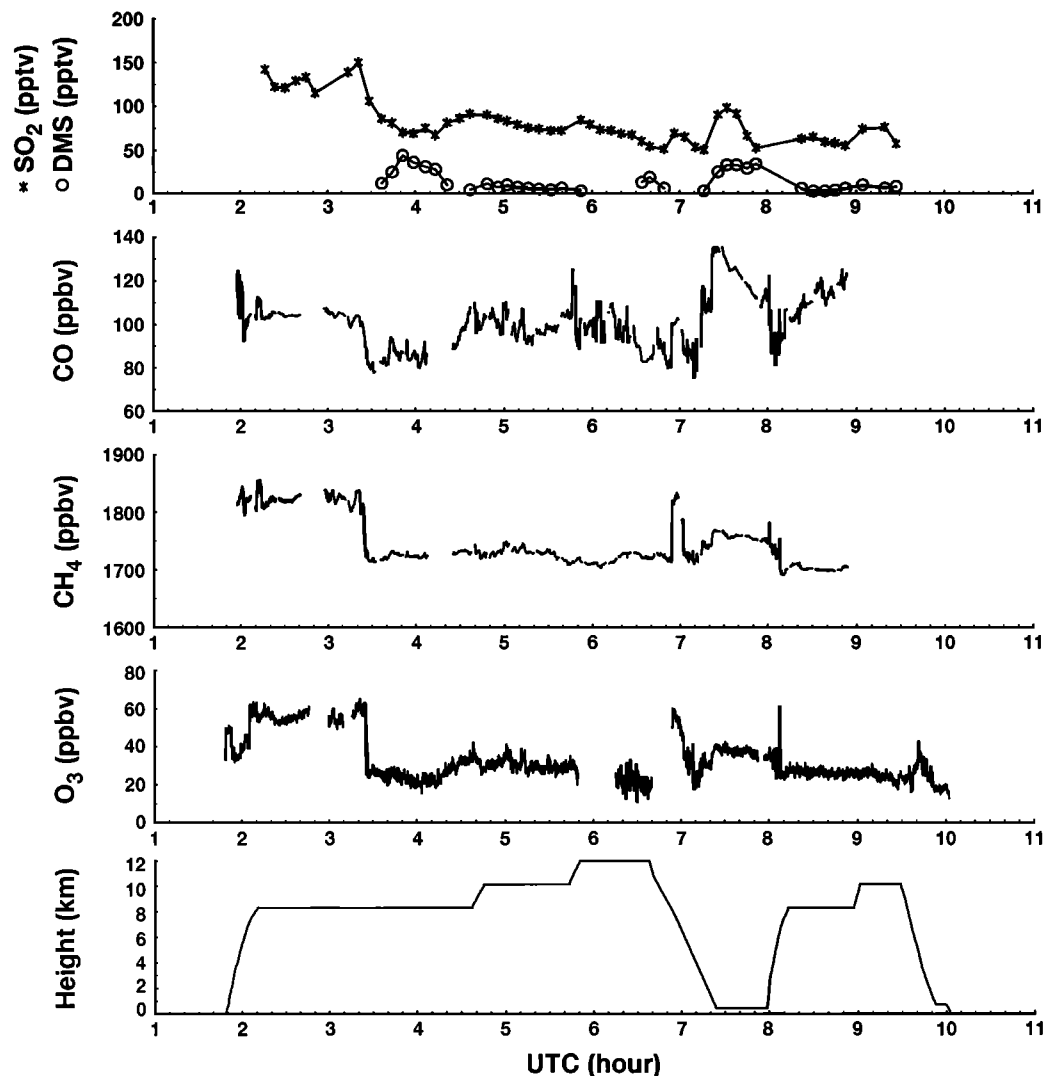


Figure 17. Time series of SO_2 (pptv), DMS (pptv), CO (ppbv), CH_4 (ppbv), O_3 (ppbv), and DC-8 altitude (km) for flight 14 on October 8, 1991.

Orchid (18.5°N , 134.0°E at 0000 UT, October 6) intensified to typhoon strength during the day as it moved slowly westward. A quasi-stationary front, oriented southwest-northeast from southern Taiwan to just south of Japan, was the boundary between the continental air mass moving eastward and southward off the Asian continent and the marine air mass over the western and central North Pacific (Figure 12h). The large cyclonic circulation of Typhoon Orchid was well defined over the Philippine Sea and was beginning to draw low-level air from Japan and Korea southward into the system.

The subtropical anticyclone covered a large portion of the western and central North Pacific (Figure 13h). In addition, a weaker anticyclonic circulation was evident along the southern China coast. Off-continent flow aloft was weak along the southern China coast, but the westerly flow off the eastern China coast was stronger north of 30°N . High-level cirrus outflow from Typhoon Orchid had reached the area just southeast of Okinawa.

Flight 14; October 8, 1991 (0148-1002 UT)

Flight 14 was a transit/survey flight from Hong Kong to Guam. During this flight the outflow from Typhoon Orchid was sampled. An anticyclone remained over central China but was weakening.

Typhoon Orchid (10.4°N , 130.4°E at 0000 UT, October 8) and Typhoon Pat (17.3° , 151.3°E at 0000 UT, October 8) were beginning to move northwestward and accelerate. The boundary between the continental air mass moving eastward and southward off the Asian continent and the cyclonic flow of marine air around Typhoon Orchid was becoming diffuse and difficult to define as a frontal feature (Figure 12i).

An anticyclone aloft along the southern China coast was responsible for weak off-continent flow over that region (Figure 13i). The deep cyclonic circulations associated with Typhoons Orchid and Pat were eroding the well-defined ridge of high pressure which had persisted over the central North Pacific during the previous month.

Patches of low- and middle-level clouds (cumulus, stratocumulus, altocumulus) were over the South China Sea and to the south of Taiwan. Extensive cloudiness associated with Typhoons Orchid and Pat was prominent over much of the western North Pacific, with clusters of organized convection located between the two storms. Based on the motion of cirrus clouds on satellite imagery loops, the outflow aloft appeared to be along the southern quadrants of both typhoons.

This flight encountered several major synoptic systems, includ-

ing passing within 300 km of the center of Typhoon Orchid. As was the case for Typhoon Mireille [Newell *et al.*, this issue], DMS was higher in the upper troposphere (44 pptv at 8.5 km, near 18.5°N, 129°E, at 0350 UT) than in the boundary layer (34 pptv at 400 m, near 17.5°N, 128.6°E, at 0730 UT, see Figure 17). There was also a sharp boundary revealed by CO, CH₄, O₃, and SO₂ at about 18.5°N, 126.0°E (0330 UT) that correlated with the wind analysis, in the sense that the rotational wind component before this time appeared to have come from the north and was of continental origin, whereas after this time the flow was part of the circulating vortex and appears to have originated further south (Figure 13i). The presence of high CO, CH₄, and O₃ together argues against stratospheric air. Another interesting observation later in the flight is the low O₃ values (> 40 ppbv) in the 11- to 16-km region as seen on DIAL (Plate 2) and the corresponding low PV ($2-4 \times 10^{-7} \text{ K m}^2 \text{ kg}^{-1} \text{ s}^{-1}$, see Plate 3). Low O₃ in tandem with low PV suggests that boundary layer air had been fairly recently lifted into the upper troposphere by deep convection.

Flight 15; October 10-11, 1991 (2351-0729 UT)

Flight 15 was a local flight southeast of Guam. As Typhoons Orchid and Pat began moving northeastward across the western North Pacific, a weak anticyclone began building over the region south of Guam (Figure 12j). These features were responsible for a low-level westerly to southwesterly flow in the vicinity of Guam and northward, but a low-level easterly to northeasterly flow existed south of about 10°S (south of the anticyclonic shear axis). Weak southerly cross-equatorial flow was evident from 150° to 160°E at the surface.

With the circulations associated with Typhoons Orchid and Pat to the north of 25°N an upper level anticyclone had become established between 10° and 15°N, leaving a light and variable flow aloft over Guam and the surrounding region (Figure 13j). A pronounced clear region associated with the anticyclonic shear axis was evident southwest of Guam. Cirrus outflow from Typhoon Pat was streaming southward and westward over the Mariana Islands and adjacent areas to the southeast. Scattered areas of deep convection southeast of Guam diminished as the day progressed. The DIAL instrument showed that low values of ozone mixing ratio were sometimes found up to high altitudes in the troposphere (~12 km), often in the form of layers which could have been produced by convective processes, as discussed elsewhere [Newell *et al.*, this issue].

Flight 16; October 13, 1991 (0039-0813 UT)

Flight 16 was a local flight from Guam to the southwest. A weak ridge anticyclone remained over Guam and the Mariana Islands. The anticyclonic shear axis was oriented southwest to northeast across that region, with westerly to southwesterly flow to the north and easterly to northeasterly flow to the south of the axis (Figure 12k). Weak southerly cross-equatorial flow was again found at the surface to the south and southeast of Guam (140° to 160°E) and also to the southwest of Guam (120°-130°E). Anticyclonic flow aloft was dominant over the tropical western Pacific. The 300-hPa flow was light and variable across the region (Figure 13k). Areas of organized convection associated with the Inter-Tropical Convergence Zone (ITCZ) generally were found between 5°-10°N, 140°-160°E. Except for cumulus clouds below the trade wind inversion, it was generally clear in the vicinity of Guam and southwestward toward the Philippines.

The aircraft performed a slow descent south of the Philippines from 9.3 to 0.7 km during the period 0332-0411 UT, corresponding to a vertical velocity of about 3.8 m s^{-1} , somewhat less than the

normal ascent rate of a rawinsonde balloon. At this rate the whole air samples collected in pressurized canisters could be collected with sufficient frequency to show the fine scale structure on vertical profiles of ethane and fluorocarbon F-12 (Figure 18). A sharp layer, about 0.5 km thick, occurs at about 1 km altitude in ethane, while F-12 (with its long lifetime) is well mixed and gives a good indication of the reliability of the sampling. These species appear to have drifted into the flight region from the east as shown by trajectories and wind cross sections (not shown). The profile shown in Figure 18 is typical of the layered structure found in the tropics [Newell *et al.*, this issue].

Flight 17; October 14-15, 1991 (1810-0208 UT)

Flight 17 was a local flight from Guam to the northwest. An anticyclone located over the central North Pacific and a weak equatorial cyclone south of Guam were responsible for a low-level easterly flow across the Mariana Islands region (Figure 12l). An anticyclonic flow regime persisted aloft over the tropical western Pacific, with light and variable flow over much of the flight region (Figure 13l).

A large well-organized cluster of convection was active to the east and northeast of Guam (in the region 15°-20°N, 145°-155°E). Of particular interest was a layer of low ozone (> 20 ppbv) at 11-12 km (Plate 4) where mixing ratios were similar to those in the boundary layer. Winds at the level of this layer were from the east-northeast, as was the motion of precipitation echoes detected by weather radar at Guam AFB. It therefore seems reasonable that this convection to the northeast may have been responsible for the formation of the elevated low-ozone layer.

Flight 18; October 17-18, 1991 (2343-0337 UT)

Flight 18 was the transit/survey flight from Guam to Wake Island. An extensive anticyclone occupied much of the western and central North Pacific, and an elongated cyclone was located south of the Mariana Islands. These two features were responsible for an easterly to northeasterly flow across much of the flight region (Figure 12m). In the upper troposphere a cyclonic shear axis was oriented southwest-northeast just north of the flight region, producing a southwesterly flow between Guam and Wake Island (Figure 13m).

An extensive area of cloudiness with embedded convection covered the region immediately south of Wake Island, between 15°-20°N, 160°-170°E. Upper level diffluence coupled with low-level convergence over that region created a favorable environment for the formation of this cloudiness. Otherwise, the remainder of the flight region between Guam and Wake Island was free from any significant cloud features.

Flight 19; October 18-19, 1991 (2202-0338 UT)

Flight 19 was the transit/survey flight from Wake Island to Honolulu, Hawaii. The dominant synoptic features were two anticyclones, one over the western North Pacific, and the other over the eastern North Pacific. A trough of low pressure was located between these two highs, with an associated weak cold frontal system oriented southwest-northeast across the central North Pacific. The southernmost extent of the front was near 25°N, or just north of the flight region. Another weak trough of low pressure (the remnants of a decaying frontal system) was located just northwest of the Hawaiian Islands. Low-level flow was generally easterly to northeasterly between Wake Island and Hawaii (Figure 12n).

A broad upper level trough covered much of the central North Pacific. As a result, cyclonic flow was found across the flight

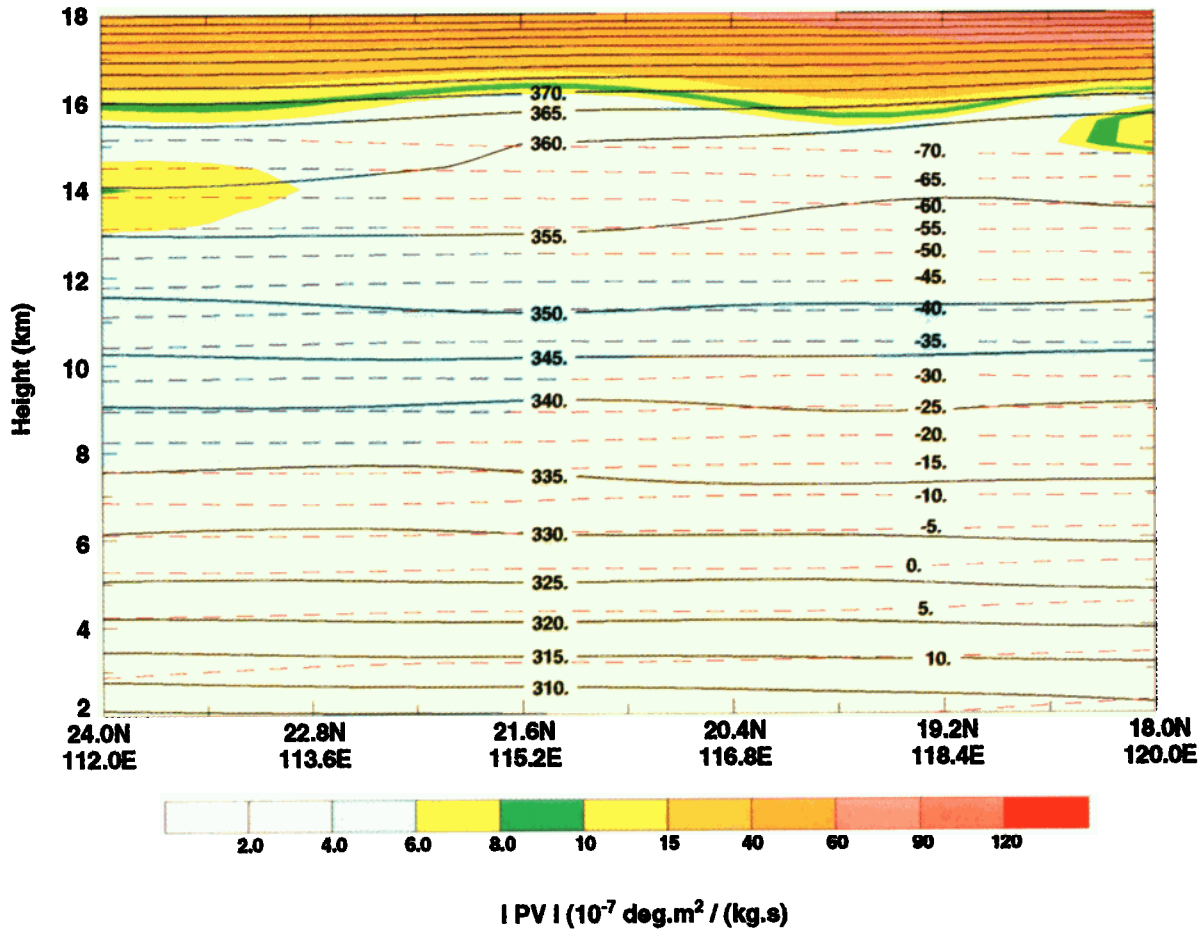


Plate 3. Cross-section of potential vorticity ($10^{-7} \text{ K m}^2 \text{ kg}^{-1} \text{ s}^{-1}$), potential temperature (solid, °K), and temperature (dashed, °C) at 0000 UT, October 8, 1991.

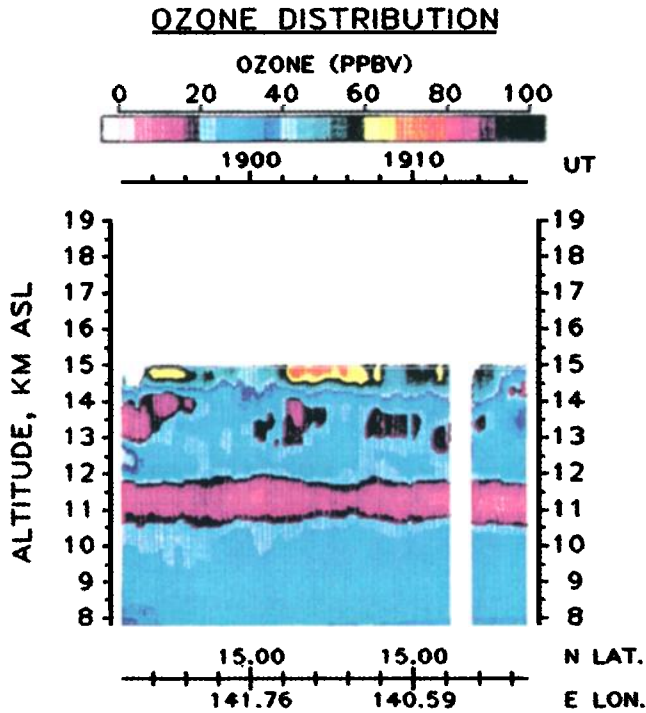


Plate 4. Cross section of relative aerosol scattering and ozone mixing ratio (ppbv) from DIAL during flight 17 on October 14, 1991.

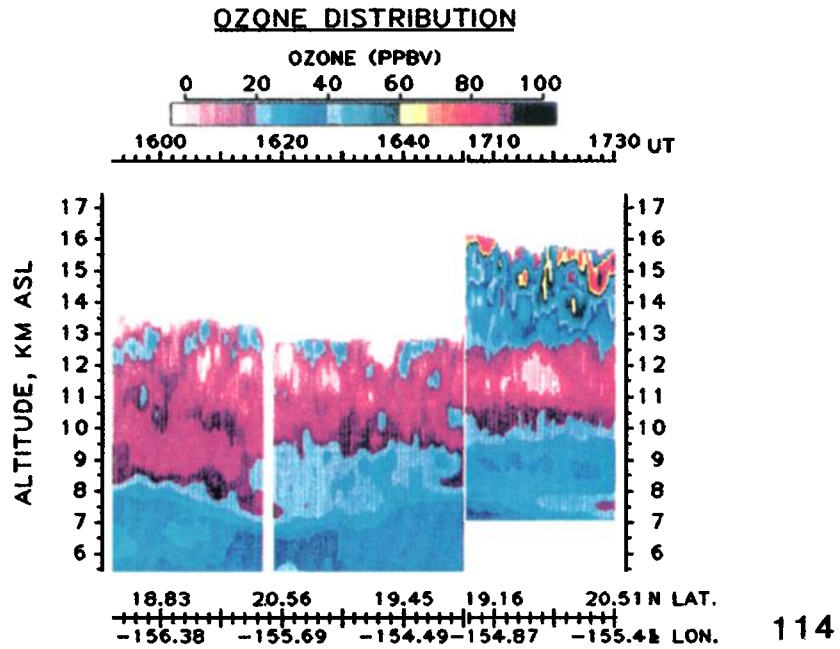


Plate 5. Cross sections of relative aerosol scattering and ozone mixing ratio (ppbv) from DIAL during flight 20 on October 20, 1991.

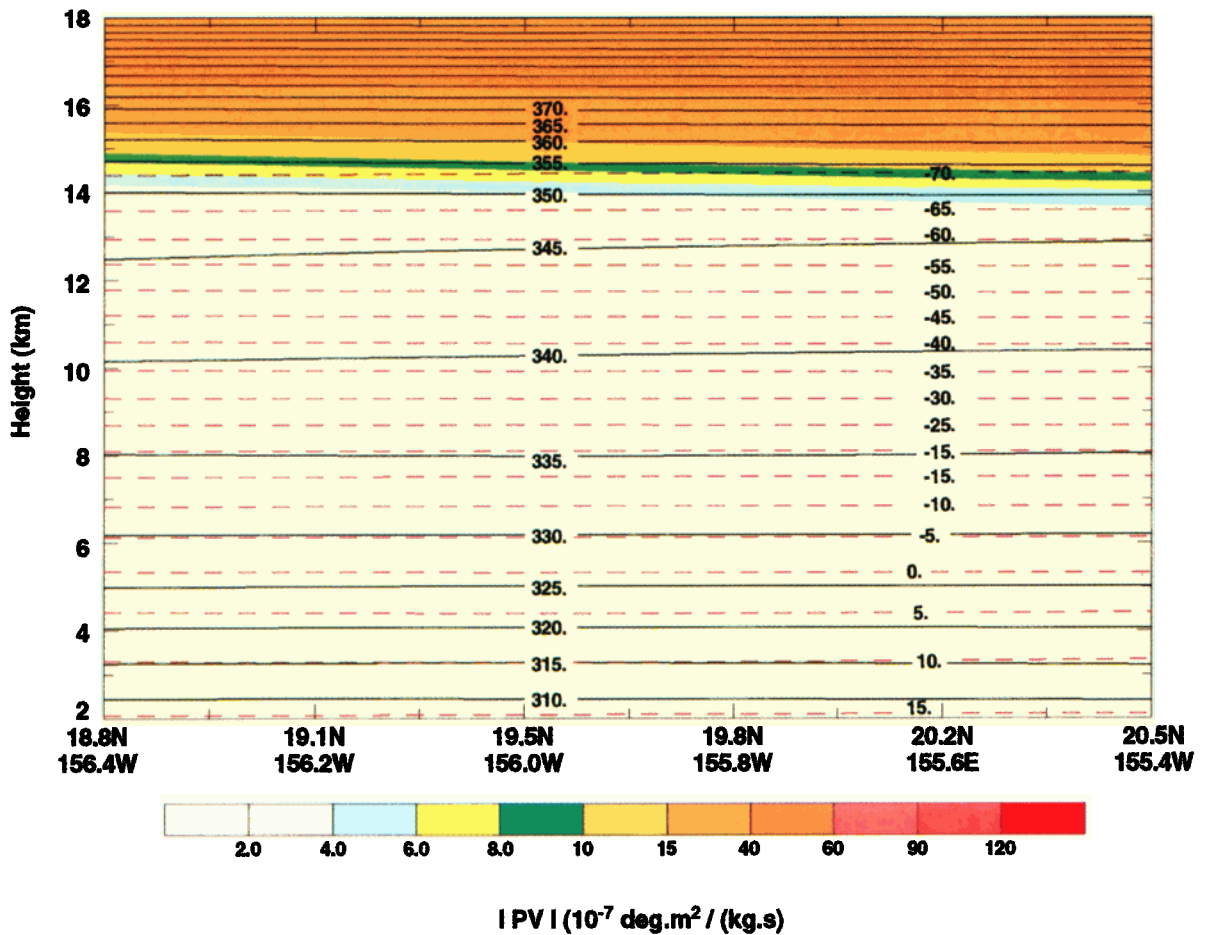


Plate 6. Cross section of potential vorticity ($10^{-7} \text{ K m}^2 \text{ kg}^{-1} \text{ s}^{-1}$), potential temperature (solid, $^{\circ}\text{K}$), and temperature (dashed, $^{\circ}\text{C}$) at 0000 UT on October 21, 1991.

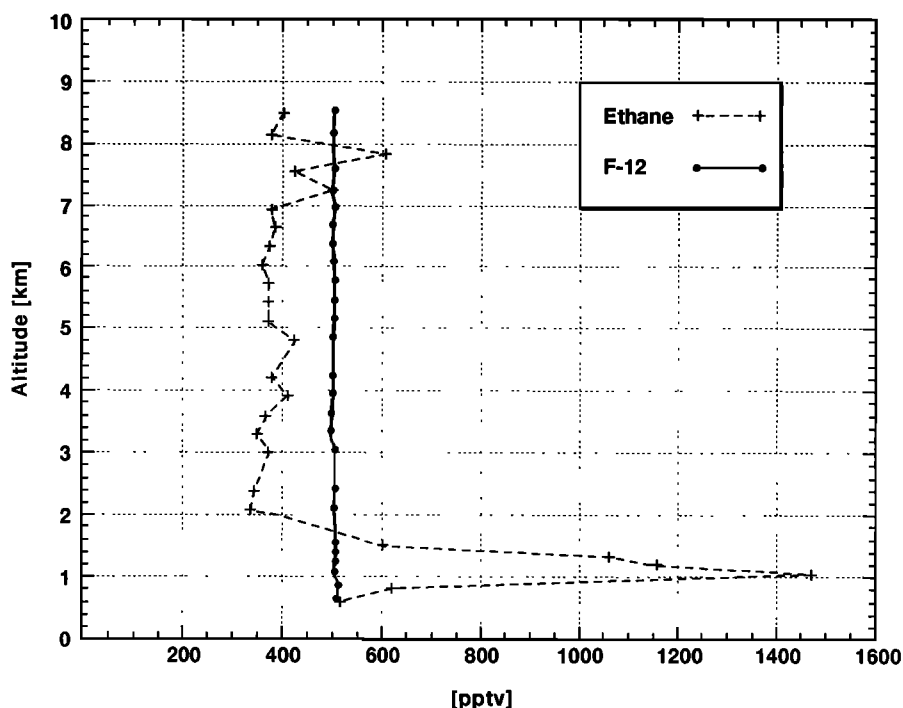


Figure 18. Vertical profile of C_2H_6 (ethane) (pptv) and CCl_2F_2 (F-12) (pptv) near $4^\circ N$, $125^\circ E$ from 0332 to 0411 UT on October 13, 1991. Data provided by F. S. Rowland and D. R. Blake, UC-Irvine.

region, with north to northeasterly flow in the vicinity of Wake Island, turning to westerly and southwesterly flow toward the Hawaiian Islands (Figure 13n).

A small area of clouds with embedded convection was over the Wake Island region. Layered clouds with convection were evident along the trough just west of the Hawaiian Islands. Along the flight track were patchy low- and middle-level clouds.

Flight 20; October 20, 1991 (1347-1947 UT)

Flight 20 was a local flight from Hawaii designed to compare a wide range of measurements aboard the DC-8 with a similar suite of ongoing measurements at the National Oceanic and Atmospheric Administration (NOAA) observatory on Mauna Loa. The measurements at Mauna Loa were part of Mauna Loa Observatory Photochemistry Experiment (MLOPEX 2), a collaborating project during the PEM-West A study. A large anticyclone remained over the eastern North Pacific, bringing an easterly flow to the Hawaiian Islands region (Figure 12o). An anticyclone aloft was centered over the Hawaiian Islands (Figure 13o). As a result, upper tropospheric winds were light and variable over the flight region. The flow patterns encountered during the flight were further complicated by the local island-induced flow effects.

The rawinsonde profile at Hilo, Hawaii indicated that the base of the trade wind inversion was between 750 hPa and 800 hPa (2-2.5 km Mean Sea Level (MSL)). Satellite imagery showed patchy low-level clouds (trade wind cumulus) to the northeast of Mauna Loa. This flight documented another good example of very low O_3 (> 20 ppbv) in the upper troposphere as measured by DIAL (Plate 5) which again corresponded to a layer of low PV (> $1 \times 10^{-7} K m^2 kg^{-1} s^{-1}$, see Plate 6).

Flight 21; October 21-22, 1991 (1932-0112 UT)

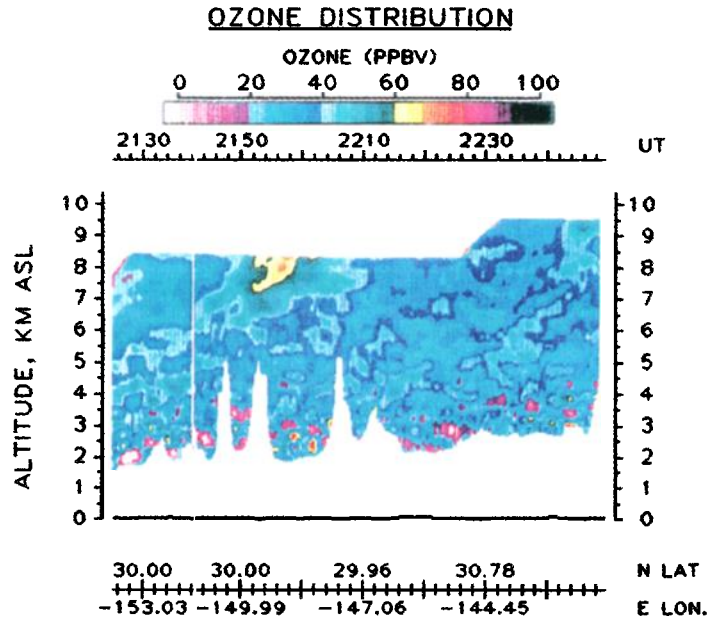
Flight 21 was the final transit/survey flight from Honolulu, Hawaii, to Moffett Field, California. An extensive anticyclone con-

tinued to dominate across the eastern North Pacific and was responsible for a northeasterly low-level flow across much of the flight region. A weak cyclonic circulation (the remnants of tropical depression Marty) had become quasi-stationary over the region between 15° - $25^\circ N$, 145° - $150^\circ W$ (Figure 12p). A cold front was moving southward along the west coast of the United States.

A north-south anticyclonic axis aloft was oriented along $160^\circ W$, while a weak cutoff cyclonic circulation was located near $28^\circ N$, $140^\circ W$. A strong short-wave trough was propagating southeastward along the west coast of North America (Figure 13p). On this occasion a PV maximum to the northeast of Hawaii had been evident for several days on isentropic PV maps supplied to us in the field by European Centre for Medium-Range Weather Forecasts (ECMWF). A GOES water vapor image obtained prior to takeoff (not shown) depicted a pronounced dry band (indicating strong subsidence in the middle and upper troposphere) to the northeast of Hawaii, and the flight was programed to traverse this feature. Stratospheric air was intercepted at 10 km around 2200 UT (near $30^\circ N$, $150^\circ W$), as indicated by in situ ozone mixing ratios near 100 ppbv; similar values (near 70 ppbv) occurred below the aircraft flight level, as detected by DIAL (Plate 7). This interpretation is further supported by a PV cross section (Plate 8), showing a protrusion of high PV into the middle troposphere. Aircraft winds showed that a strong flow from the north accompanied these high O_3 values, indicating a jet streak along the western periphery of the cutoff cyclonic feature (Figure 13p).

7. Conclusions

A brief description of the synoptic situation for each of the PEM-West A missions has been presented. In addition, meteorological data have been used to give background information for some of the more marked atmospheric trace constituent features observed. In particular, in several cases where stratosphere-to-



119

Plate 7. Cross section of relative aerosol scattering and ozone mixing ratio (ppbv) from DIAL during flight 21 on October 21, 1991.

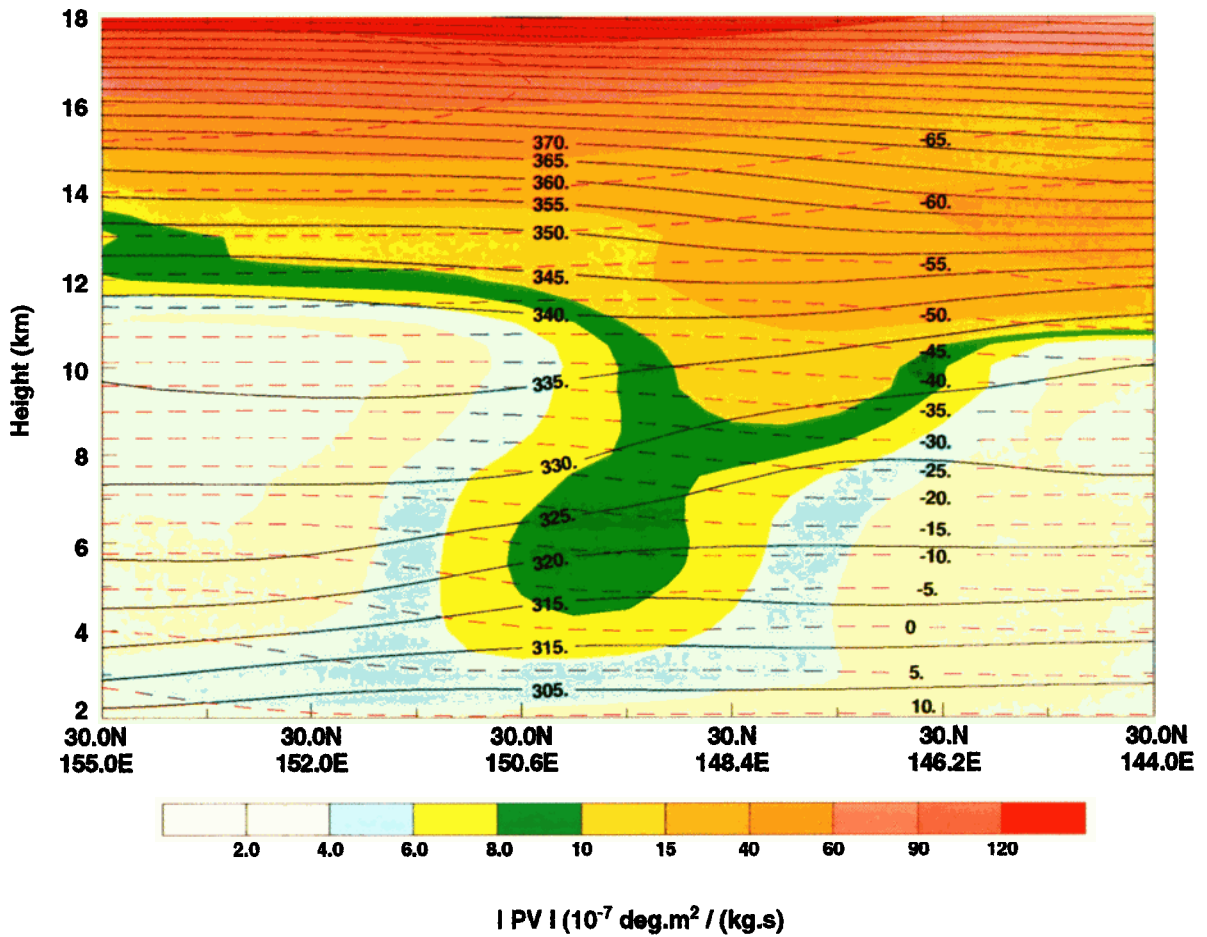


Plate 8. Cross section of potential vorticity ($10^{-7} \text{ K m}^2 \text{ kg}^{-1} \text{ s}^{-1}$), potential temperature (solid, °K), and temperature (dashed, °C) for 0000 UT on October 22, 1991.

troposphere exchange was suspected, comparisons were made between the DIAL ozone and PV cross sections, which were found to support the explanation. Three cases where boundary layer air was found within the middle to upper troposphere have been identified by virtue of DIAL low ozone together with low PV. Two more cases were found from the flights through Typhoons Mireille and Orchid, where the identification of boundary layer air was made from in situ observations of DMS at nearly the same mixing ratios in the boundary layer and in the upper troposphere. From a total flying time above 6 km of 60 hours, 5.6 hours (about 9%) had values of DMS greater than one quarter of the boundary layer values on the same flight. This is a rough measure of the fraction of time the boundary layer was in communication with the upper troposphere; some distortion exists because flights were often planned to avoid active storm areas. Several of these constituent features are treated in detail in papers that follow in this volume, and the topic of layering is also explored further.

Acknowledgment. The authors would like to recognize the invaluable assistance and kind hospitality of the staff of the Hong Kong Royal Observatory. Thanks are also extended to Frank Mewszel, who spent many long hours getting the GMS ground station operational. In the field we were helped by the reception of daily faxes from ECMWF containing isentropic PV maps and forecast trajectories for each mission. ECMWF also provided their model grid point analysis data after the mission. John Merrill provided isentropic trajectories during and after the mission. Air Force forecasters at Honolulu, Guam, and Yokota were helpful in contributing their local knowledge and forecasting advice. At Guam we received much practical aid from C. P. Guard, Frank Wells, and Mark Lander; their knowledge and experience covered the whole Pacific. During the flights we received substantial cooperation from the flight deck crews and mission managers so that the sampling could be adjusted to the meteorological situation, often in close to real time. Donald Blake and Sherwood Rowland (University of California-Irvine) provided NMHC data for Figure 18, Donald Thornton and Alan Bandy (Drexel Univ.) provided sulfur components of Figure 10 and Plate 3, Gerald Gregory and Bruce Anderson (NASA Langley) provided O₃ data in Figures 12 and 17, and Glen Sachse and James Collins Jr. (NASA Langley) provided CO and CH₄ data in Figures 10 and 17. Susan Walters prepared the final versions of many of the figures.

References

- Arimoto, R., et al., Relationships among aerosol constituents from Asia and the North Pacific during PEM-West A, *J. Geophys. Res.*, this issue.
- Bachmeier, A. S., M. C. Shipham, E. V. Browell, W. B. Grant, and J. M. Klassa, Stratospheric/tropospheric exchange affecting the northern wetlands region of Canada during summer 1990, *J. Geophys. Res.*, **99**, 1793-1804, 1994.
- Browell, E. V., et al., Large-scale air mass characteristics observed over the western Pacific during the summertime, *J. Geophys. Res.*, this issue.
- Carlson, T. N., The evolution of cyclones, in *Midlatitude Weather Systems*, pp. 221-264, Harper Collins Acad., London, 1991.
- Danielsen, E. F., Stratospheric source for unexpectedly large values of ozone measured over the Pacific during GAMETAG, August 1977, *J. Geophys. Res.*, **85**, 401-412, 1980.
- Danielsen, E. F., and R. S. Hipskind, Stratospheric-tropospheric exchange at polar latitudes in summer, *J. Geophys. Res.*, **85**, 392-400, 1980.
- Gregory, G. L., A. S. Bachmeier, D. R. Blake, B. G. Heikes, D. C. Thornton, J. D. Bradshaw, and Y. Kondo, Chemical signatures of aged Pacific marine air: Mixed layer and free troposphere as measured during PEM-West A, *J. Geophys. Res.*, this issue.
- Hoell, J. M., D. D. Davis, S. C. Liu, R. Newell, M. Shipham, H. Akimoto, J. McNeal, R. J. Bendura, and J. W. Drewry, Pacific Exploratory Mission-West A (PEM-West A): September-October 1991, *J. Geophys. Res.*, this issue.
- Janowiak, J. E., The global climate for September-November 1991: Warm (ENSO) episode conditions strengthen, *J. Clim.*, **6**, 1616-1638, 1993.
- Merrill, J. T., Trajectory results and interpretation for PEM-West A, *J. Geophys. Res.*, this issue.
- Merrill, J. T., M. Uematsu, and R. Bleck, Meteorological analyses of long range transport of mineral aerosol over the North Pacific, *J. Geophys. Res.*, **94**, 8584-8598, 1989.
- Newell, R. E., et al., Atmospheric sampling of supertyphoon Mireille with the NASA DC-8 aircraft on September 27, 1991 during PEM-West A, *J. Geophys. Res.*, this issue (a).
- Newell, R. E., Z.-X. Wu, Y. Zhu, W. Hu, E. V. Browell, G. L. Gregory, G. W. Sachse, J. E. Collins Jr., K. K. Kelly, and S. C. Liu, Vertical fine-scale atmospheric structure measured from the NASA DC-8 during PEM-West A, *J. Geophys. Res.*, this issue (b).
- Newell, R. E., Y. Zhu, E. V. Browell, W. G. Read, and J. W. Waters, Walker circulation and upper tropospheric water vapor, *J. Geophys. Res.*, this issue (c).
- Newell, R. E., Y. Zhu, E. V. Browell, S. Ismail, W. Read, J. Waters, K. Kelly, and S. Liu, Upper tropospheric water vapor and cirrus: Comparison of DC-8 observations, preliminary UARS MLS measurements, and meteorological analyses, *J. Geophys. Res.*, this issue (d).
- Prospero, J. M., M. Uematsu, and D. L. Savoie, 1989. Mineral aerosol transport to the Pacific Ocean, In J. P. Riley, R. Chester, and R. A. Duce, eds., *Chemical Oceanography*, Vol. 10-SEAREX: The Sea/Air Exchange Program. Academic Press, London, England, pp. 187-218.
- Royal Observatory, Hong Kong, (ROHK), *Tropical Cyclones in 1991*, Gov. Publ. Cent., 1993.
- Rudolf, D. K., and C. P. Guard, *1991 Annual Tropical Cyclone Report*, 238 pp., Joint Typhoon Warning Cent., Guam, 1992.
- Talbot, R. W., et al., Chemical characteristics of continental outflow from Asia to the troposphere over the western Pacific Ocean during September-October 1991: Results from PEM-West A, *J. Geophys. Res.*, this issue.
- Thornton, D. C., A. R. Bandy, B. W. Blomquist, D. D. Davis, and R. W. Talbot, Sulfur dioxide as a source of CN in the upper troposphere of the Pacific Ocean, *J. Geophys. Res.*, this issue.
- A. S. Bachmeier (corresponding author), Lockheed Engineering and Sciences Company, 144 Research Drive, Hampton, VA 23666
- R. E. Newell and Y. Zhu, Massachusetts Institute of Technology, Cambridge, MA 02138
- E. V. Browell and M. C. Shipham, Atmospheric Sciences Division, NASA Langley Research Center, Hampton, VA 23681-0001
- D. R. Blake, University of California, Irvine, CA 92717

(Received August 8, 1995; revised September 10, 1995; accepted September 10, 1995.)